

Predicting Out-of-Domain Generalization with Neighborhood Invariance

Nathan Ng

University of Toronto

Vector Institute

Massachusetts Institute of Technology

nathanng@mit.edu

Neha Hulkund

Massachusetts Institute of Technology

nhulkund@mit.edu

Kyunghyun Cho

New York University

Prescient Design, Genentech

CIFAR Fellow

kyunghyun.cho@nyu.edu

Marzyeh Ghassemi

Massachusetts Institute of Technology

CIFAR AI Chair

Vector Institute

mghassem@mit.edu

Reviewed on OpenReview: <https://openreview.net/forum?id=jYkWdJzTun>

Abstract

Developing and deploying machine learning models safely depends on the ability to characterize and compare their abilities to generalize to new environments. Although recent work has proposed a variety of methods that can directly predict or theoretically bound the generalization capacity of a model, they rely on strong assumptions such as matching train/test distributions and access to model gradients. In order to characterize generalization when these assumptions are not satisfied, we propose neighborhood invariance, a measure of a classifier’s output invariance in a local transformation neighborhood. Specifically, we sample a set of transformations and given an input test point, calculate the invariance as the largest fraction of transformed points classified into the same class. Crucially, our measure is simple to calculate, does not depend on the test point’s true label, makes no assumptions about the data distribution or model, and can be applied even in out-of-domain (OOD) settings where existing methods cannot, requiring only selecting a set of appropriate data transformations. In experiments on robustness benchmarks in image classification, sentiment analysis, and natural language inference, we demonstrate a strong and robust correlation between our neighborhood invariance measure and actual OOD generalization on over 4,600 models evaluated on over 100 unique train/test domain pairs.

1 Introduction

As deep neural networks find increasing use in safety-critical domains such as autonomous driving (Gupta et al., 2021) and healthcare (Wiens et al., 2019), it is important to develop methods to understand and compare how these models generalize to new environments. Although empirically these models generalize in many settings (Hendrycks et al., 2020a; Allen-Zhu et al., 2018; Neyshabur et al., 2017a), they also exhibit numerous failure cases. For example, models have been shown to overfit to a dataset’s meta characteristics (Recht et al., 2019) or arbitrarily corrupted labels (Zhang et al., 2016), learn spurious correlations (Liang

arXiv:2207.02093v3 [cs.LG] 17 Jul 2023

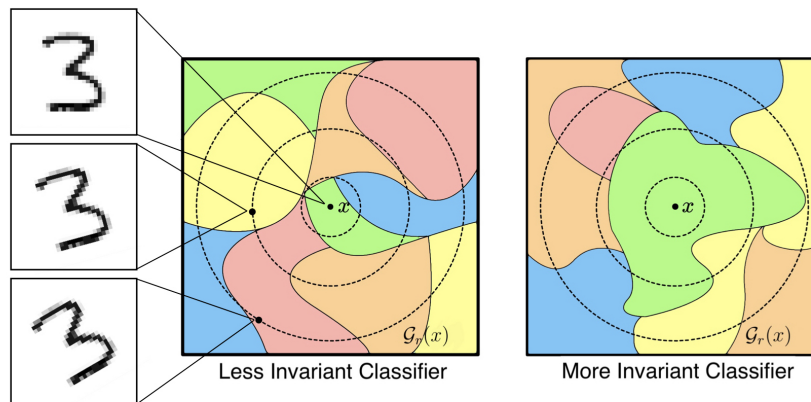


Figure 1: The transformation neighborhood $\mathcal{G}_r(x)$ around x contains the set of points reachable from a transformation in \mathcal{G}_r (pictured here as a rotation of r degrees). As r increases, the transformation neighborhood is partitioned into a distinct set of decision regions. More invariant classifiers (right) classify most points in the neighborhood into the same class and should generalize better compared to less invariant classifiers (left). Our measure of invariance is independent of what specific region x lies in.

& Zou, 2022), and change their predictions even with small adversarial perturbations (Goodfellow et al., 2014; Papernot et al., 2017). Many methods have been proposed to mitigate these issues, but precisely characterizing the generalization properties of a model in diverse settings remains an open problem.

One line of work aims to theoretically bound generalization capacity (Vapnik & Chervonenkis, 1971; Bartlett & Mendelson, 2003; McAllester, 1999; Neyshabur et al., 2017a; Dziugaite & Roy, 2017; Neyshabur et al., 2015b) or directly predict generalization (Keskar et al., 2016; Liang et al., 2019; Neyshabur et al., 2015a; Schiff et al., 2021; Jiang et al., 2019), and are useful in reasoning about a model beyond its performance on a specific known test set. However, these methods work only when train and test distributions are the same, and often rely on a strong set of assumptions such as access to labelled test data (Schiff et al., 2021), model weights (Neyshabur et al., 2015b; Bartlett et al., 2017; Neyshabur et al., 2017b), model gradients (Jiang et al., 2019), and training data (Keskar et al., 2016). More recent work aims to estimate the generalization of a trained model on unlabelled test data directly (Deng & Zheng, 2021; Jiang et al., 2021; Deng et al., 2021; Garg et al., 2022). However, these metrics are typically calculated based on the output logits of a model on individual examples, which can become poorly calibrated in out-of-domain (OOD) settings (Morteza & Li, 2022). In real world settings, we require a robust measure of generalization that can be applied across a wide range of test distributions and where we are often given access only to a black box model.

In this paper we propose *neighborhood invariance*, a complexity measure that correlates well with generalization and that only assumes access to a set of suitable data transformations. Given a test data point, we define the transformation neighborhood as the set of points that can be generated from a set of transformations with a given maximum magnitude. A classifier’s neighborhood invariance is then the proportion of points that are classified into the most commonly predicted class in this neighborhood. Intuitively, a classifier that is more invariant in this neighborhood should be able to represent examples with lower dimensionality and thus lower complexity, leading to stronger generalization. Different from other similar methods (Aithal K et al., 2021), we define invariance with respect to the neighborhood itself rather than relative to the prediction at the test point and do not require manually tuning weights, meaning our measure can be applied even when test distributions vary. In addition, since our measure makes so few assumptions it is applicable in a wide range of experimental settings and can be used to compare the generalization properties of multiple models even when labeled data is unavailable.

We investigate the correlation of a model’s neighborhood invariance with its capacity to generalize, focusing on experimental settings with OOD dataset shifts (Taori et al., 2020) where test data is sampled from a

distribution different from the training distribution. We select common OOD benchmark datasets in image classification (Krizhevsky, 2009; Lu et al., 2020; Recht et al., 2018; Deng, 2012; Darlow et al., 2018; Netzer et al., 2011; Arjovsky et al., 2019; Taori et al., 2020), sentiment analysis (Ni et al., 2019), and natural language inference (Williams et al., 2018), which totals over 100 pairs of training/test domains. We consider a large pool of over 4,600 models trained on these datasets with varying architectures and generalization properties, and sample sets of transformations commonly used for data augmentation (Ng et al., 2020; Cubuk et al., 2020; Wei & Zou, 2019; Xie et al., 2019). Across a wide set of correlation metrics, we find that neighborhood invariance measures outperform or match baselines in almost all experimental settings.

2 Related Work

Characterizing Model Invariance Ensuring various kinds of model invariance is a well studied aspect of learning generalizable models and has been analyzed extensively from a causality perspective (Bühlmann, 2018; Peters et al., 2015; Haavelmo, 1943). At the largest scale, models trained on a wide support of training data and domains have demonstrated robust zero-shot and few-shot abilities (Radford et al., 2021; Brown et al., 2020; Wortsman et al., 2022). At a smaller scale, models that are invariant across data domains or interventions (Arjovsky et al., 2019; Gulrajani & Lopez-Paz, 2020; Bühlmann, 2018) are able to learn representations that do not depend on spurious correlations. Finally, at the smallest scale, local invariance to data augmentations (Cubuk et al., 2020), local changes (Rifai et al., 2011), augmentation graphs (HaoChen et al., 2021), similar neighbors (Luo et al., 2018), or interpolation between points (Verma et al., 2019; Zhang et al., 2018) have demonstrated improvements in model generalization. In our paper, we consider model invariance at this local scale.

Recent work has shown that models that are invariant to local transformations factorize the input space into a base space and the set of transformations (Sokolić et al., 2017; Sannai et al., 2021), effectively reducing the input dimensionality and thus model complexity (Anselmi et al., 2016; Anselmi et al., 2015). Measuring this decrease in complexity can be performed by analyzing the sample cover (Zhu et al., 2021). A similar line of work derives estimation error bounds based on the intrinsic dimensionality of deep ReLU networks in Hölder (Schmidt-Hieber, 2019; Nakada & Imaizumi, 2020; Chen et al., 2019), Besov, mixed smooth Besov (Suzuki, 2018), and anisotropic Besov (Suzuki & Nitanda, 2021) function spaces.

Most similar to our work, Aithal K et al. (2021) measures a model’s robustness to perturbations as a proxy for generalization. Our method generalizes theirs and differs in a few key ways. We calculate our measure on the test set relative to a transformation neighborhood and can thus adapt to any specific domain for which we measure complexity and predict generalization. In contrast, Aithal K et al. (2021) calculate their measure on the training set, use the models’ prediction as a ground truth, and require manually tuning the weights of augmentations, meaning it is relatively brittle and can only be applied to in-domain data. In addition we analyze the correlation of our neighborhood invariance measure on a wide range of OOD benchmarks on image classification, sentiment analysis, and natural language inference, while Aithal K et al. (2021) consider only image classification tasks with matching train/test distributions.

Measures of Complexity and Predicting Generalization Traditional methods of analyzing the generalization bounds of neural networks use theoretical measures of complexity. VC dimension (Vapnik & Chervonenkis, 1971) and Rademacher complexity (Bartlett & Mendelson, 2003) can be used to bound the generalization of particular function classes, although they are often vacuous at the scale of deep neural networks (Dziugaite & Roy, 2017). The PAC-Bayes framework (McAllester, 1999; Neyshabur et al., 2017a; Dziugaite & Roy, 2017; Garg et al., 2021) can be used to build tighter generalization bounds by considering the “sharpness” of the local minima. Norm-based measures (Neyshabur et al., 2015b; Bartlett et al., 2017; Neyshabur et al., 2017b) bound generalization by considering different norms of the weights of learned networks. More recent analyses have focused on empirically motivated measures that do not provide theoretical bounds. These include the sharpness of minima in parameter space Keskar et al. (2016), Fisher-Rao norm Liang et al. (2019), distance from initialization (Nagarajan & Kolter, 2019), path norm (Neyshabur et al., 2015a), layer margin distributions (Jiang et al., 2019), and perturbation response curves Schiff et al. (2021).

However, these measures are only applicable when train and test distributions match. Although some generalization bounds have been derived for these OOD settings (Garg et al., 2021; Ben-David et al., 2007;

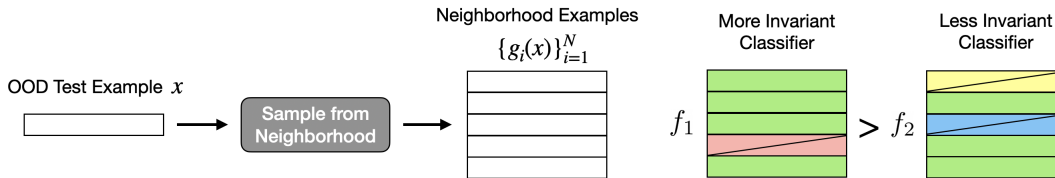


Figure 2: To estimate neighborhood invariance we sample a set of transformations $\{g_i\}_{i=1}^N \sim \mathcal{G}_r$ and generate a set of nearby examples $\{g_i(x)\}_{i=1}^N$ for every test example x . This set of examples is then evaluated using each classifier. We expect classifiers with more points classified in the most common class to generalize better to the given test set.

Zhang et al., 2019), they rely on access to the test data distribution. In addition, many testbeds examine only synthetic shifts, whereas natural shifts such as WILDS (Koh et al., 2021) are much more difficult. In real world settings where test distributions are often unknown, a separate line of work aims to directly predict generalization from unlabelled test data. These methods either predict the correctness on individual examples (Deng & Zheng, 2021; Jiang et al., 2021; Deng et al., 2021), directly estimate the total error (Garg et al., 2022; Guillory et al., 2021; Chen* et al., 2021; Chuang et al., 2020; Vedantam et al., 2021), or learn linear models relating ID and OOD accuracy (Miller et al., 2021) or agreement (Baek et al., 2022).

3 Neighborhood Invariance Measure

In this section we introduce our neighborhood invariance measure. We start by defining the transformation neighborhood of a point, then motivate our formulation of invariance in this neighborhood, and finally show how to estimate it in practice.

3.1 Motivation

Consider a classification task from an input space \mathcal{X} to an output space \mathcal{Y} with k classes. We are given a model $f : \mathcal{X} \rightarrow \mathcal{Y}$ trained on an in-domain training dataset $\mathcal{D}_i = \{(x_i^1, y_i^1), \dots, (x_i^n, y_i^n)\}$ sampled from a distribution $P_i(\mathcal{X}, \mathcal{Y})$, and an out-of-domain test dataset $\mathcal{D}_o = \{(x_o^1, y_o^1), \dots, (x_o^m, y_o^m)\}$ sampled from a distribution $P_o(\mathcal{X}, \mathcal{Y})$. We assume further that domains are covariate shifted such that $P(\mathcal{Y}|\mathcal{X})$ does not change between domains

We consider a set of data transformations $\mathcal{G}_r = \{g : \mathcal{X} \rightarrow \mathcal{X} \mid m(g) < r\}$ where g is a particular data transformation with an associated measure of the magnitude of the transformation $m(g)$. For example, a set of image rotation transformations with a maximum angle of 30 degrees might be denoted \mathcal{G}_{30} where $m(g_i) = \alpha$ is the angle of rotation for a specific g_i . For a given test point $x \in \mathcal{D}_o$, we define the transformation neighborhood $\mathcal{G}_r(x) = \{g(x) \in \mathcal{X} \mid g \in \mathcal{G}_r\}$ as the set of outputs after applying all transformations in \mathcal{G}_r . Defining the neighborhood this way allows us to consider a wide range of nearby points in a controllable way without needing access to the underlying data distribution. As shown in Figure 1, for a given r , we can define a neighborhood decision distribution as

$$p_j(x) = \frac{|\{f(x') = j \mid x' \in \mathcal{G}_r(x)\}|}{|\mathcal{G}_r(x)|}. \quad (1)$$

We then define our **neighborhood invariance measure** as

$$\mu(f, x) = \max_{j \in \mathcal{Y}} p_j(x). \quad (2)$$

We assume that data transformations are selected such that the label for the transformed point $g(x)$ is still well defined. For example, flipping MNIST digits horizontally would cause most examples to have an undefined label. If the label is undefined, then $f(g(x))$ should produce close to random outputs and thus

constant invariance values of $1/k$ regardless of the generalization properties of f , causing our measure to fail. We empirically measure this phenomenon across a wide range of transformations in Section 5.4.

Intuitively, a classifier that is more invariant in the neighborhood of x should be able to represent it with a lower input dimensionality and thus be less complex, leading to stronger generalization capabilities. In contrast, a less invariant classifier will need a higher input dimensionality to represent the neighborhood of x and thus be more complex, leading to weaker generalization. Crucially, since our invariance is measured with respect to the neighborhood around the test point rather than the test point itself, it does not rely on the ground truth label. In addition, it makes no assumptions about the model or the distribution from which test data was sampled, making it applicable in many settings where existing complexity measures cannot be calculated, including common OOD robustness settings.

3.2 Estimating Neighborhood Invariance

Calculating neighborhood invariance exactly is typically intractable since evaluating all possible transformations is impossible. Instead, we perform Monte Carlo estimation by sampling a set of N transformations $\{g_i\}_{i=1}^N$ from \mathcal{G}_r (including the identity transformation $I(x) = x$) and calculating

$$\mu(f, x) = \frac{1}{N} \sum_{i=1}^N \mathbb{1}(f(g_i(x)) = \hat{y}(f, x)), \quad (3)$$

where

$$\hat{y}(f, x) = \arg \max_{j \in \mathcal{Y}} \sum_{i=1}^N \mathbb{1}(f(g_i(x)) = j) \quad (4)$$

is the most commonly output label. The average neighborhood invariance across the entire dataset \mathcal{D}_o is then $\frac{1}{m} \sum_{j=1}^m \mu(f, x_o^j)$.

4 Experimental Setup

Empirically evaluating the quality of a complexity measure is difficult and requires careful experimental design. Typically, evaluation is done by generating a large pool of models with sufficiently varied generalization properties, but if we generate these models by varying only a few hyperparameters, our observed correlation may be an artifact of these factors affecting both generalization and our measure. To this end, we follow a similar experimental setup to Jiang et al. (2019).

4.1 Data

For our experiments we focus on three tasks: large and small scale image classification, sentiment analysis on single sentences and natural language inference on sentence pairs. For each task we construct a set of datasets sampled from different data domains.

Image Classification For image classification we begin by considering 7 datasets domain shifted from ImageNet (Deng et al., 2009; Russakovsky et al., 2015) These include ImageNetV2 (Recht et al., 2019) and Imagenet-Sketch (Wang et al., 2019) with the same output classes, as well as ObjectNet (Barbu et al., 2019), ImageNetVid, YTBB anchors (Gu et al., 2019; Recht et al., 2019), ImageNet-A (Hendrycks et al., 2021b), and ImageNet-R (Hendrycks et al., 2021a) with a smaller subset of output classes.

In addition to ImageNet datasets we construct two sets of smaller scale datasets. The first we call **CI10** and consists of CIFAR10 (Krizhevsky, 2009), CINIC10 (Darlow et al., 2018), CIFAR10.1(Recht et al., 2018), and CIFAR10.2(Lu et al., 2020). The second we call **Numbers** and consists of SVHN (Netzer et al., 2011), MNIST (Deng, 2012), and Colored MNIST (Arjovsky et al., 2019). Domains in each set share the same set of output classes.

Sentiment Analysis (SA) We use the datasets subsampled from the Amazon reviews dataset (Ni et al., 2019) which contains product reviews from Amazon. Following Hendrycks et al. (2020b) and Ng et al. (2020),

Model	Dataset	Training Domain	Batch Size	Depth	Width	Dropout	Weight Decay	Label Noise	Learning Rate	Batch Norm	Seed	Data Aug	# Converged	# Evaluations
CNN	Amazon	10	3	3	3	3	3	—	—	—	—	—	2,418	24,180
	MNLI	5	3	3	3	2	—	3	—	—	—	—	796	39,800
RoBERTa	Amazon	10	3	—	—	2	3	3	—	—	—	—	332	33,200
	MNLI	5	3	—	—	2	3	3	—	—	—	—	213	10,650
Various	ImageNet	—	—	—	—	—	—	—	—	—	—	—	401	2,406
NiN	SVHN	—	3	3	—	3	2	—	—	—	—	—	54	162
	CIFAR10	—	2	2	2	2	2	—	—	—	—	—	32	128
VGG	CIFAR10	—	3	3	—	3	2	—	—	—	—	—	54	216
ResNet	CIFAR10	—	—	—	3	—	3	—	2	2	3	2	216	864
CNN	CINIC10	—	2	2	4	—	2	—	2	2	—	—	128	512
													4,644	112,118

Table 1: Number of possible hyperparameter values for each architecture and task. Fields denoted with a — indicate that this hyperparameter is fixed or not applicable. We also list the total number of models converged and evaluations run in each model pool. In total we consider 4,644 models and 112,118 evaluations.

we split the dataset into 10 different domains based on review category. For all domains and datasets, models are trained to predict a review’s star rating from 1 to 5.

Natural Language Inference (NLI) We use the MNLI (Williams et al., 2018) dataset, a corpus of NLI data from 10 distinct genres of written and spoken English. We train on the 5 genres with training data and evaluate on all 10 genres. Models are given two sentences, a premise and hypothesis, and predict whether the hypothesis is entailed by, is neutral to, or contradicts the premise.

4.2 Model and Hyperparameter Space

For large scale image classification on ImageNet, we use pretrained models from the ImageNet Testbed (Taori et al., 2020) which covers a wide range of architectures including ResNext (Xie et al., 2016), EfficientNet (Tan & Le, 2019), BiT (Beyer et al., 2021), Vision Transformers (Dosovitskiy et al., 2020), CLIP (Radford et al., 2021), and many more models. We provide a full list of models evaluated in Appendix A.2. For smaller scale image classification tasks, we use models trained for the tasks 1, 2, 4, 5, and 9 from the Predicting Generalization in Deep Learning competition (PGDL) (Jiang et al., 2020) as well as models from Jiang et al. (2019), which covers Network in Network (NiN) (Lin et al., 2013), VGG (Simonyan & Zisserman, 2015), ResNet (He et al., 2015), and CNN models trained on CIFAR10, CINIC10, and SVHN. On natural language tasks we consider CNN (Kim, 2014; Mou et al., 2016) and RoBERTa (Liu et al., 2019) based models. On natural language models we apply label noise by randomly replacing a fraction of training labels with uniform samples from the label space. We argue that label noise is not an artificial training setting as stated in Jiang et al. (2019) but rather a method of entropy regularization (Pereyra et al., 2017; Xie et al., 2016) which prevents models from becoming overconfident.

In order to control for the varying convergence rates and learning capacities of our different models, we follow Jiang et al. (2019) and early stop the training of models when they reach a given training cross entropy loss (usually around 99% training accuracy), or if they reach the max number of training epochs. We discard all models which do not converge within this time. The total number of models trained and converged in each pool as well as details on hyperparameter variations for each task and model provided in Table 1. We include further details on model training, the hyperparameter space, and specific choices in hyperparameters in Appendix A.4, A.2, and A.3.

4.3 Evaluation Metrics

Given a set of domains defined by distributions $\{P_1, P_2, \dots, P_n\}$ and a set of datasets $\{\mathcal{D}_i \sim P_i\}_{i=1}^n$ sampled from these domains, we train a set of models $F_i = \{f_i^1, f_i^2, \dots, f_i^m\}$ on each dataset \mathcal{D}_i . We evaluate all models $f_i^k \in F_i$ on all OOD test datasets $\mathcal{D}_o : o \neq i$, generating a set of invariance and generalization values (μ_{io}^k, g_{io}^k) . We define generalization as the top-1 accuracy of f_i^k on \mathcal{D}_o .

We evaluate our measure first by predicting the generalization of a given model to an OOD test set. Specifically, we select an OOD test set \mathcal{D}_o and an in-domain training set $\mathcal{D}_i : i \neq o$ and predict the OOD generalization g_{io}^k

of a model f_i^k trained on \mathcal{D}_i and evaluated on \mathcal{D}_o from its invariance value μ_{io}^k . To generate these predictions we use a linear model $\hat{g} = a\mu + b$ with parameters $a, b \in \mathcal{R}$. To estimate our parameters a and b , we select a pool of models $\{f_j^k \in F_j : j \neq i, o\}$ that are trained on *all remaining datasets*. Each model f_j^k in this pool is evaluated on the OOD dataset \mathcal{D}_o to give us a set of pairs $\{(\mu_{jo}^k, g_{jo}^k)\}$. We then find a, b by minimizing the mean squared error $(a^*, b^*) = \arg \min_{a,b} \sum_{j,k} (a\mu_{jo}^k + b - g_{jo}^k)^2$ on all models in the pool.

We use the learned parameters to make generalization predictions $\hat{g}_{io}^k = a\mu_{io}^k + b$ for every model $f_i^k \in F_i$ on \mathcal{D}_o and measure the coefficient of determination \mathbf{R}^2 (Glantz et al., 1990). We also measure the residuals of our linear model by calculating the mean absolute error (**MAE**) between our predictions and the actual generalization. For every pair of training domain i and OOD test domain o , we evaluate R^2 and MAE then average each metric across all pairs. We report MAE values as percentage points.

We also consider the rank correlation between neighborhood invariance and actual generalization. Specifically, for a pair of models f_i, f_j with measure and generalization pairs (μ_i, g_i) and (μ_j, g_j) , we want $g_i > g_j$ if $\mu_i > \mu_j$. We use Kendall’s rank τ coefficient (Kendall, 1938) to measure how consistent these sets of rankings are. We measure four different τ values:

ID τ This metric evaluates the correlation of our measure with in-domain generalization. We select a training dataset \mathcal{D}_i and consider pairs $\{(\mu_{ii}^k, g_{ii}^k)\}$ generated from the set of models F_i trained on \mathcal{D}_i . τ values are averaged across all training domains.

Macro τ This metric evaluates the correlation of our measure individually on each training/OOD test domain pair. We select a training dataset \mathcal{D}_i and a OOD test dataset \mathcal{D}_o and consider pairs $\{(\mu_{io}^k, g_{io}^k)\}$ generated from the set of models F_i trained on \mathcal{D}_i . τ values are averaged across all pairs of training and OOD test domains.

Micro τ This metric evaluates the correlation of our measure on a given OOD test domain across models trained on all other domains. We select a single OOD test domain \mathcal{D}_o and consider pairs $\{(\mu_{io}^k, g_{io}^k)\}$ generated from the set of models $\{f_i^k \in F_i : i \neq o\}$ trained on all other datasets $\{\mathcal{D}_i : i \neq o\}$. τ values are averaged across all test domains. We use this metric only when different models are trained on different training sets.

Arch τ This metric evaluates the correlation of our measure on models trained with different architectures. Arch τ is calculated similar to Micro τ , except F_i now includes models from all architectures. τ values are averaged across all test domains.

4.4 Data Transformations

Defining the transformation neighborhood requires defining a set of data transformations with associated magnitudes. For image classification, we consider four transformations: RandAugment (Cubuk et al., 2020) which randomly combines various transformations, random translation in the X- and Y-axes, random patch erasing (Zhong et al., 2020) which removes randomly sized patches from the image, and horizontal flips and crops. We call neighborhood invariance measures based on these transformations **NI-RandAug**, **NI-Translate**, **NI-Erase**, and **NI-FC** respectively. For natural language tasks, we also consider four transformations: SSMBA (Ng et al., 2020) which generates examples in a manifold neighborhood using a denoising autoencoder, EDA (Wei & Zou, 2019) which applies random word level operations, backtranslation (BT) (Rico Sennrich, 2016; Xie et al., 2019) which translates back and forth from a pivot language, and a transformation that randomly replaces a percentage of tokens. We call neighborhood invariance measures based on these transformations **NI-SSMBA**, **NI-EDA**, **NI-BT**, and **NI-RandRep** respectively. For all experiments we sample $n = 10$ transformations in addition to the identity transformation, although ablations in section 5.4 show that our method is relatively robust to the specific number of transformations sampled. We provide further details on specific transformation magnitude values and implementations for all methods in Appendix A.5.

4.5 Baselines

Since our experimental setting makes so few assumptions, there are very few complexity measures that we can compare against. This includes Aithal K et al. (2021), which requires matching train/test distributions.

We thus consider complexity measures that require only model weights, specifically the **Spectral** (Yoshida & Miyato, 2017; Neyshabur et al., 2017b) and **Frobenius** (Neyshabur et al., 2015b) norms. However, in our experiments we find close to 0 or negative correlation for these measures, so we do not report their performance. We also compare our method against output based methods that directly predict OOD generalization. We use **ATC-MC** and **ATC-NE** Garg et al. (2022) as our two baselines, which calculate a threshold on in-domain validation data based on max confidence and negative entropy scores respectively. To calculate metrics on these methods we treat the generated accuracy predictions as a score. To calculate ID τ values we select a threshold value based on validation data then calculate predicted accuracy values on test data from the same domain. For ImageNet domain shift datasets where the output classes are a subset of the original 1,000 ImageNet classes, we do not recompute a subclassed ATC threshold as we do not assume prior knowledge of the OOD output classes.

5 Results

We now present the results of our experiments evaluating the quality of our neighborhood invariance measure. We begin by analyzing the effect of dataset distance on the correlation of neighborhood invariance with generalization in a toy setting. Our main set of results evaluate neighborhood invariance on OOD benchmarks in image classification, sentiment analysis, and natural language inference. Finally, we examine the correlation of our measure in extreme OOD settings and analyze the factors that affect the quality of our neighborhood invariance estimates.

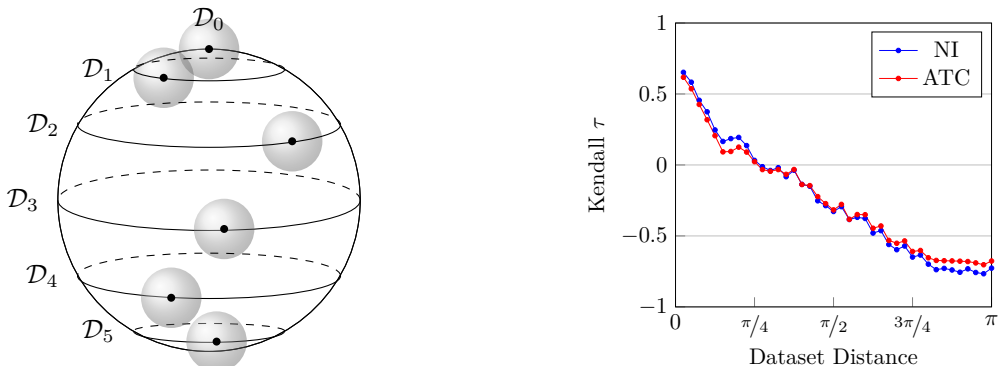
5.1 Dataset Distance: Toy Analysis

In general, as with any complexity measure or generalization predictor, we expect neighborhood invariance to perform more poorly as we move farther from the training domain. In the worst case, if a classifier becomes a degenerate constant classifier in a far enough OOD domain, then neighborhood invariance reaches a constant maximum value of 1 while generalization becomes random. In order for our measure to work well, we assume that test domains are sufficiently close to training domains so that model predictions are non-constant. In this section we present an analysis of the effect of dataset distance on the quality of our measure in a toy setting.

We consider a binary classification task of points inside and outside a unit hypersphere in $\mathcal{X} = \mathcal{R}^n$, as shown in Figure 2. We define different data domains as univariate gaussian distributions $P(\mathcal{X})$, centered at a point μ on the hypersphere. The distance between two datasets $\mathcal{D}_1 \sim P_1(\mathcal{X})$ and $\mathcal{D}_2 \sim P_2(\mathcal{X})$ can then be measured as the distance along the hypersphere between μ_1 and μ_2 in radians. We generate a training dataset \mathcal{D}_0 by sampling points around the north pole of the hypersphere, then generate out-of-domain datasets \mathcal{D}_j at varying distances from \mathcal{D}_0 . Given a model trained on \mathcal{D}_0 , we can calculate its generalization to \mathcal{D}_j , as well as its neighborhood invariance.

In our experiments, we consider a 16 dimensional hypersphere and sample 1000 points per data distribution for each dataset. The univariate gaussian distributions that we sample data points from have fixed variance 0.005, ensuring models cannot generalize fully across the entire hypersphere. We train 200 single hidden-layer MLPs with hidden dimension of 16 on the training dataset \mathcal{D}_0 , each with a random level of label noise between 0-30% to ensure a wide range of generalization properties. We consider 40 different dataset distances, equally spaced along the hypersphere between opposite poles. For a given dataset distance, we select 5 points at random from the corresponding circumference and generate 5 datasets from univariate gaussians centered at these points. To measure neighborhood invariance for a given x , we sample 10 transformations from the set of transformations defined as a perturbation along the hypersphere of radius $\|x\|$ with a maximum distance $m(g) = \|g(x) - x\| \leq 0.01$. For each dataset we measure the neighborhood invariance and generalization for each of the 200 trained models and calculate the Kendall τ correlation between them. For a given dataset distance, the τ values are then averaged across all datasets. Results are presented in Figure 3b.

For datasets closest to the training dataset, the correlation between generalization and neighborhood invariance is high. However, as dataset distance increases, correlation decreases. At a distance of around $\pi/4$, correlation becomes nearly 0, and continues decreasing until the two values are negatively correlated on data sampled



(a) We generate data from univariate gaussians whose means lie on a hypersphere. We train models on a dataset \mathcal{D}_0 to classify points as inside or outside the hypersphere then test them on out of domain datasets \mathcal{D}_j that lie at various distances from \mathcal{D}_0 as measured by radian distance along the hypersphere.

(b) The correlation between neighborhood invariance and OOD generalization remains high near the training domain but quickly decreases as dataset distance increases, becoming negatively correlated for datasets further than $\pi/4$ away on the hypersphere. We observe almost identical results for baseline ATC methods.

Figure 3: Toy analysis of the effect of dataset distance on the correlation between neighborhood invariance and OOD generalization.

from the opposite side of the hypersphere from the training domain. This behavior almost identical for both neighborhood invariance and ATC methods (ATC-MC and ATC-NE perform the same so we report only one). These results demonstrate that the correlation of neighborhood invariance with generalization should decrease as dataset distance increases. To investigate the degree to which this happens in practice, we consider a set of extreme OOD experiments (Section 5.3) where we observe a surprisingly small decrease in correlation, indicating a closer dataset distance than might initially be assumed.

5.2 Correlation with OOD Generalization

We first present results in Table 2 analyzing the correlation of our proposed neighborhood invariance measure with OOD generalization. We report R^2 , MAE, Macro τ , Micro τ , ID τ , and Arch τ as detailed in Section 4.3. We omit results on Spectral and Frobenius norm measures as they are close to 0 or negative for all metrics. We do not report Micro τ values for image classification models since each model type is trained on only one domain. Additional experiments and results are presented in Appendix B.

ImageNet-Scale Image Classification Results on ImageNet-scale image classification datasets are presented in Table 2a and are averaged across all architectures. On standard domain shifts, NI-RandAug performs slightly better than ATC methods on R^2 and Macro τ with similar MAE. On the adversarial ImageNet-A dataset, ATC methods fail completely whereas NI methods maintain strong performance and still correlate well with accuracy. However, both methods exhibit large MAE and fail to accurately predict actual OOD accuracy. On ID τ NI methods perform slightly worse than ATC methods although they still show very strong correlations.

CIFAR10-Scale Image Classification Results on smaller scale image classification datasets are presented in Table 2b and are averaged across all architectures. On CI10 datasets, NI-RandAug significantly outperforms ATC baselines and all other measures on all metrics. NI-RandAug also exhibits only a small decrease in correlation when moving from in-domain (ID τ) to OOD datasets (Macro τ), compared to ATC methods which suffer a much larger drop. On Numbers datasets, NI-RandAug outperforms all other methods on R^2 and MAE, although it performs slightly worse on Macro τ compared to NI-Translate and on ID τ compared to ATC baselines.

For both CI10 and Numbers, using patch erasing and flip and crop transformations cause our method to perform worse or fail entirely, in contrast to ImageNet where they perform similarly or better. For these

Measure	Domain Shifts			ImageNet-A			
	R^2	MAE	Macro τ	R^2	MAE	Macro τ	ID τ
NI-RandAug	0.709	11.87	0.724	0.577	31.17	0.586	0.845
NI-Translate	0.587	13.58	0.604	0.468	29.54	0.439	0.834
NI-Erase	0.492	11.86	0.555	0.446	33.06	0.517	0.803
NI-FC	0.603	12.28	0.691	0.679	31.84	0.589	0.867
ATC-NE	0.607	11.40	0.703	0.209	32.00	0.248	0.931
ATC-MC	0.622	11.97	0.691	0.159	32.85	0.190	0.942

(a) Results on ImageNet scale models and datasets. On standard domain shift datasets NI-RandAug performs slightly better than ATC methods, and maintains strong performance on adversarial data where ATC methods fail completely.

Measure	CI10					Numbers			
	R^2	MAE	Macro τ	ID τ	Arch τ	R^2	MAE	Macro τ	ID τ
NI-RandAug	0.899	3.11	0.768	0.793	0.837	0.764	5.33	0.642	0.733
NI-Translate	0.732	3.56	0.607	0.661	0.786	0.685	6.12	0.667	0.881
NI-Erase	0.518	4.41	0.411	0.406	0.299	0.153	10.17	-0.135	0.324
NI-FC	0.417	4.47	0.371	0.344	0.683	0.208	10.42	-0.316	-0.033
ATC-NE	0.655	3.61	0.548	0.693	0.689	0.616	6.74	0.637	0.859
ATC-MC	0.640	3.65	0.544	0.682	0.685	0.692	6.19	0.682	0.844

(b) Results on small scale image classification, averaged across all model architectures. No Micro τ is reported since models are trained on a single domain and no Arch τ is reported for the Numbers dataset since we only consider a single architecture. NI-RandAug beats all other methods on almost all metrics.

Measure	CNN					RoBERTa					
	R^2	MAE	Macro τ	Micro τ	ID τ	R^2	MAE	Macro τ	Micro τ	ID τ	Arch τ
NI-SSMBA	0.662	1.93	0.677	0.689	0.629	0.972	1.29	0.832	0.829	0.838	0.588
NI-EDA	0.641	2.04	0.664	0.649	0.611	0.968	1.45	0.830	0.810	0.830	0.512
NI-BT	0.550	2.99	0.592	0.501	0.538	0.961	1.47	0.813	0.801	0.801	0.523
NI-RandRep	0.409	2.64	0.544	0.554	0.439	0.967	1.27	0.821	0.816	0.822	0.537
ATC-NE	0.760	2.47	0.514	0.633	0.467	0.852	2.38	0.707	0.691	0.749	0.660
ATC-MC	0.761	2.46	0.517	0.634	0.467	0.869	2.26	0.722	0.705	0.749	0.663

(c) Results on sentiment analysis (SA) datasets. NI-SSMBA beats all other methods on almost all metrics.

Measure	CNN					RoBERTa					
	R^2	MAE	Macro τ	Micro τ	ID τ	R^2	MAE	Macro τ	Micro τ	ID τ	Arch τ
NI-SSMBA	0.575	2.09	0.570	0.534	0.704	0.933	1.19	0.750	0.730	0.771	0.301
NI-EDA	0.577	2.04	0.581	0.511	0.709	0.941	1.26	0.789	0.757	0.799	0.572
NI-BT	0.509	2.11	0.470	0.449	0.584	0.944	1.07	0.759	0.740	0.778	0.563
NI-RandRep	0.451	2.20	0.452	0.428	0.570	0.890	1.70	0.688	0.647	0.710	0.401
ATC-NE	0.576	2.52	0.568	0.446	0.705	0.737	2.22	0.557	0.541	0.739	0.635
ATC-MC	0.576	2.52	0.568	0.446	0.706	0.769	2.10	0.581	0.567	0.748	0.636

(d) Results on natural language inference (NLI) datasets. NI measures beat baselines on all metrics except Arch τ .

Table 2: Evaluation metrics measuring the correlation of our neighborhood invariance measure with ID/OOD generalization. The best performing measures for each metric are bolded. On all tasks, neighborhood invariance achieves strong generalization and beats baseline methods on almost all metrics. Full tables for R^2 , Macro τ , Micro τ , and ID τ on individual train/test domains are in Appendix C

Measure	CNN		RoBERTa	
	R^2	Micro τ	R^2	Micro τ
NI-SSMBA	0.584	0.566	0.941	0.816
NI-EDA	0.575	0.567	0.884	0.715
NI-BT	0.538	0.470	0.906	0.766
NI-RandRep	0.277	0.373	0.918	0.776
ATC-NE	0.271	0.495	0.329	0.356
ATC-MC	0.295	0.506	0.437	0.436

(a) Results on the `Drugs.com` dataset.

Measure	CNN		RoBERTa	
	R^2	Micro τ	R^2	Micro τ
NI-SSMBA	0.083	0.080	0.691	0.463
NI-EDA	0.202	0.110	0.739	0.540
NI-BT	0.213	0.247	0.730	0.527
NI-RandRep	0.096	0.102	0.030	0.012
ATC-NE	0.077	-0.107	0.719	0.345
ATC-MC	0.076	-0.106	0.734	0.354

(b) Results on the MedNLI dataset.

Table 3: Evaluation metrics measuring the correlation of our neighborhood invariance measure with generalization on extreme OOD datasets. NI-* methods beat baselines on both tasks, with RoBERTa models exhibiting only a slight degradation in correlation compared to more typical OOD settings.

smaller datasets, since these transformations are more likely to generate images that cannot be classified (e.g. images without an object in frame), they produce more similar invariance values between classifiers that cannot be used to rank them properly. This effect is more pronounced for Numbers datasets because flipping the image or removing even small portions of the number to be classified can render the task impossible. In contrast, random image translation which almost always preserves label information performs similarly well across both datasets and almost matches NI-RandAug. We provide a larger set of ablations on the Numbers dataset exploring this phenomenon in Section 5.4. The strong performance of NI-RandAug indicates that combining multiple transformations is helpful for mitigating dataset-specific transformation sensitivities, as in the case of Numbers.

Sentiment Analysis (SA) Results on Sentiment Analysis datasets are presented in Table 2c. In experiments on both architectures, our neighborhood invariance measures achieve strong correlation with OOD generalization and beats all baselines on almost all metrics. Of the transformations considered, NI-SSMBA performs the best across both architectures. NI-EDA, NI-BT, and even NI-RandRep achieve strong results as well, often beating ATC baselines. We observe particularly strong correlation on RoBERTa models, with a nearly perfectly linear R^2 value of 0.972 and large Micro τ of 0.829. We hypothesize that this is due to the pretrained initialization of RoBERTa models, which gives a strong inductive bias towards learning a space invariant to transformations that preserve meaning. In contrast, CNN models are trained from random initializations and may not learn as closely aligned a space. On cross architecture analysis, we observe strong Arch τ for our neighborhood measures, although they are outperformed by both ATC methods. Compared to image classification results, our results on sentiment analysis tasks are overall less sensitive to the data transformations selected because they are less likely to destroy information necessary for classification.

Natural Language Inference (NLI) Results on Natural Language Inference tasks are presented in Table 2d. Similar to our sentiment analysis results, our neighborhood invariance measures achieve strong correlation with OOD generalization on both architectures and beat all baselines. Correlations in general on NLI are lower than those of sentiment analysis because it is more difficult to maintain the complex relationship between the two sentences during a transformation. For example, changing a single word can easily change a sentence pair from entailment to contradiction, whereas many words must be changed to modify a 5 star review to a 1 star review. We observe exceptionally high correlation on RoBERTa models, for which we offer a similar hypothesis as in our sentiment analysis experiments. On cross architecture analysis, we observe strong correlation for our NI-EDA and NI-BT although they are outperformed by both ATC methods.

5.3 Extreme OOD Generalization

We now consider more extreme generalization to data domains with specialized and knowledge intensive data. We consider only natural language tasks as it is difficult to find a sufficiently specialized image classification dataset that maintains the same output classes. For sentiment analysis we use the `Drugs.com` review dataset (Gräber et al., 2018), and for natural language inference we use MedNLI (Romanov & Shivade, 2018), an

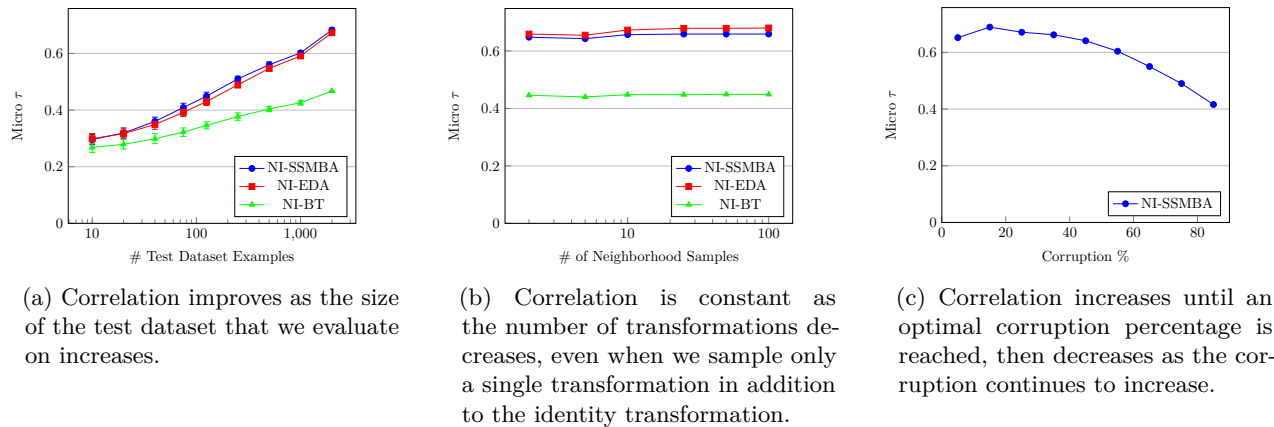


Figure 4: Micro τ for our neighborhood invariance measure calculated with varying ablations on CNN models evaluated on Amazon toy reviews.

NLI dataset generated from clinical notes and patient history. Both datasets contain highly specific medical language not seen in any of our training domains. All models from all original training domains are evaluated on each of these extreme OOD domains, and we report R^2 and Micro τ . Results are shown in Table 3

On the `Drugs.com` dataset, we observe a small decrease in correlation for neighborhood invariance methods compared to results on AWS datasets. However, ATC methods begin to fail, with Micro τ on RoBERTa models dropping significantly from 0.706 to 0.356. This suggests that models become poorly calibrated in extreme OOD settings, making ATC methods fragile. On MedNLI we observe a much larger disparity in performance. For CNN models, most of our measures fail to correlate at all, and ATC methods degrade so much they became anti correlated with generalization. For RoBERTa models we observe only minor drops in correlation for all measures. For both tasks NI-RandRep exhibits almost no correlation with OOD generalization. This suggests that the choice of transformation becomes much more important as we move farther from our training domain.

5.4 Ablations

In this section we examine factors that may affect the quality of neighborhood invariance estimation and its correlation with actual generalization. Since rerunning all of our experiments is too costly, we evaluate on toys Amazon reviews using a pool of CNN models trained on all other domains for the first three ablations, and on the Numbers datasets using NiN models trained on SVHN for the final two.

Test Dataset Size: Does our neighborhood invariance measure still correlate well when the test dataset is small? We randomly and iteratively subsample our test dataset of 2000 examples to reduce our dataset size down to 10 examples. We then measure our models’ neighborhood invariance on each subsampled dataset and calculate the Micro τ on all models. Results are shown in Figure 4a. We find that for all neighborhoods, smaller datasets lead to noisier invariance estimates and lower correlation. As dataset size increases, correlation increases as well.

Number of Transformations: How many transformations do we need to sample in order to generate a reliable neighborhood invariance estimate? We sample a varying number of transformations for each test example, from a minimum of two transformations to a maximum of 100 transformations, then estimate our neighborhood invariance measure with each set of transformations on the entire test dataset and calculate the micro τ . By default we always include the identity transformation. Results are shown in Figure 4b. We find that our measure is surprisingly robust to the number of samples, with only a small difference between 100 and 2 transformations sampled. For all measures, correlation slightly increases as the number of samples increases and we achieve a better estimation of the true invariance value.

Training Regime	R^2	MAE	Macro τ	ID τ
Standard Training	0.684	12.37	0.763	0.852
+ Augmentation/Robustness	0.707	12.23	0.650	0.855
+ Pretraining/Extra Data	0.799	11.73	0.707	0.836
All Models	0.709	11.87	0.724	0.845

Table 4: NI-RandAug results on different subsets of the ImageNet Testbed models trained with different training regimes. Training with augmentation and robustness interventions decreases macro τ compared to standard training but increases all other metrics. R^2 and MAE are higher for models trained/pretrained with large amounts of data.

Transformation Magnitude: How sensitive is our measure to the maximum magnitude of transformation considered? We use the SSMB transformation for which the magnitude of a transformation is defined by the percentage of tokens corrupted, which we vary from a minimum of 5% to a maximum of 85%. After sampling a set of transformations from each corruption level, we estimate neighborhood invariance on the test dataset using each set and calculate the micro τ on all models. Results are shown in Figure 4c. We find that as we begin to increase the corruption percentage, correlation begins to increase as well. Correlation reaches a maximum, then decreases as we continue to increase our corruption percentage. However, even at 85% corruption, our method is quite robust and achieves a micro τ of 0.416.

Selecting Transformations: How do we ensure that transformations are suitable for a given dataset and do not destroy label information? We consider the set of NiN models trained on SVHN and a set of image transformations including RandAugment (Cubuk et al., 2020), rotations, translations, shears, brightness jittering, contrast jittering, color jittering, patch erasing, and flips and crops. For each transformation and both OOD datasets ColoredMNIST and MNIST we calculate the Macro τ correlation between accuracy and neighborhood invariance, as well as the average entropy difference between a model’s output on a transformed image and on the original image. Results are shown in Figure 5.

Neighborhood invariance is relatively insensitive to the transformation selected, with most transformations performing similarly up to a certain entropy difference threshold around 0.1, after which it fails. The transformations that fail, erase and flip crop, both tend to destroy label information and lead to much higher entropy outputs. We propose this method of examining entropy differences as a simple way to diagnose whether a given transform is appropriate for a specific dataset.

Pretraining and Training with Augmentation: Does self-supervised pretraining or training with data augmentations, which should make models more invariant to certain transformations, make our neighborhood invariance measure ineffective? We begin by examining our metrics on subsets of models from the ImageNet Testbed (Taori et al., 2020) split by models trained on standard ImageNet (81 models), models trained on ImageNet with augmentations and robustness interventions (74 models), and finally models trained with extra data or pretrained with self-supervised objectives (41 models). Results are shown in Table 4. We find that compared to evaluating only on standard training models, the addition of augmentations or pretraining slightly degrades Macro τ , but improves R^2 and MAE. Compared to the overall results on all models, we do not observe any large decreases in performance.

Since the augmentations considered in the set of ImageNet Testbed models are not the same across models, we also consider models from PGDL (Jiang et al., 2020) trained with and without a single type of augmentation: flip crop. Calculating our evaluation metrics on each set of models allows us to isolate the effect of data augmentation. Results are shown in Table 5. We find that measuring neighborhood invariance using the same transformation (NI-FC) that models are trained with causes only a slight degradation compared to models trained without. When measuring invariance using other transformations (NI-RandAug, NI-Erase), evaluation metrics actually improve slightly.

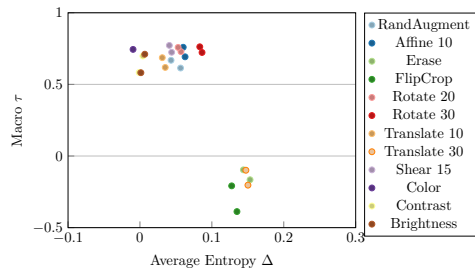


Figure 5: Transformations whose neighborhood invariance measures correlate well with OOD generalization exhibit smaller differences in output entropy.

Measure	Flip Crop	R^2	MAE	Macro τ	ID τ
NI-RandAug	✗	0.833	3.32	0.719	0.753
	✓	0.844	3.16	0.732	0.744
NI-Translate	✗	0.874	2.61	0.768	0.831
	✓	0.877	2.52	0.794	0.845
NI-Erase	✗	0.790	3.28	0.716	0.702
	✓	0.812	3.17	0.722	0.719
NI-FC	✗	0.681	4.34	0.620	0.587
	✓	0.663	4.23	0.608	0.554

Table 5: Training with and without flip crop augmentation has a minimal effect on the effectiveness of our method, even when the transformation neighborhood aligns with those used to train the model (NI-FC).

6 Discussion

In this paper, motivated by the limited settings in which existing complexity measures can be applied, we propose a simple to calculate neighborhood invariance measure that can be applied even when test distributions are unknown and model training data, weights, and gradients are unavailable. We evaluate our method on image classification, sentiment analysis, and natural language inference datasets, calculating a variety of correlation metrics with both in-domain and out-of-domain (OOD) generalization. Across almost all tasks and experimental settings, we find that our neighborhood invariance measure consistently outperforms baseline methods and correlates strongly with actual generalization. However, our method has several limitations. Data transformations must be selected such that labels for transformed points are still well defined, although examining entropy differences can diagnose poor transformation choices. In settings where such transformations are difficult to define, our method may not be applicable or provide inappropriately high estimates, so practitioners must be careful to verify their estimates with a labelled test set. In addition, our neighborhood invariance measure may fail in sufficiently OOD settings where a model may become poorly calibrated or degenerate, although we find in practice on our tasks that even extreme OOD settings are similar enough for our measure to perform well. In future work we plan to explore using similar measures calculated over transformation neighborhoods as a method for OOD detection.

7 Acknowledgments

We would like to thank Taylor Killian, Tom Hartvigsen, and Swami Sankaranarayanan for their helpful discussion and comments. Resources used in preparing this research were provided, in part, by the Province of Ontario, the Government of Canada through CIFAR, and companies sponsoring the Vector Institute (www.vectorinstitute.ai/partners).

References

- Sumukh Aithal K, Dhruva Kashyap, and Natarajan Subramanyam. Robustness to Augmentations as a Generalization metric. *arXiv e-prints*, art. arXiv:2101.06459, January 2021.
- Zeyuan Allen-Zhu, Yuanzhi Li, and Yingyu Liang. Learning and Generalization in Overparameterized Neural Networks, Going Beyond Two Layers. *arXiv e-prints*, art. arXiv:1811.04918, November 2018.
- Fabio Anselmi, Lorenzo Rosasco, and Tomaso Poggio. On Invariance and Selectivity in Representation Learning. *arXiv e-prints*, art. arXiv:1503.05938, March 2015.
- Fabio Anselmi, Joel Z. Leibo, Lorenzo Rosasco, Jim Mutch, Andrea Tacchetti, and Tomaso Poggio. Unsupervised learning of invariant representations. *Theoretical Computer Science*, 633:112–121, 2016. ISSN 0304-

3975. doi: <https://doi.org/10.1016/j.tics.2015.06.048>. URL <https://www.sciencedirect.com/science/article/pii/S0304397515005587>. Biologically Inspired Processes in Neural Computation.
- Martin Arjovsky, Léon Bottou, Ishaan Gulrajani, and David Lopez-Paz. Invariant risk minimization. *arXiv*, 2019.
- Christina Baek, Yiding Jiang, Aditi Raghunathan, and Zico Kolter. Agreement-on-the-line: Predicting the performance of neural networks under distribution shift, 2022.
- Andrei Barbu, David Mayo, Julian Alverio, William Luo, Christopher Wang, Dan Gutfreund, Josh Tenenbaum, and Boris Katz. Objectnet: A large-scale bias-controlled dataset for pushing the limits of object recognition models. In H. Wallach, H. Larochelle, A. Beygelzimer, F. d'Alché-Buc, E. Fox, and R. Garnett (eds.), *Advances in Neural Information Processing Systems*, volume 32. Curran Associates, Inc., 2019. URL https://proceedings.neurips.cc/paper_files/paper/2019/file/97af07a14cacba681feacf3012730892-Paper.pdf.
- Peter L. Bartlett and Shahar Mendelson. Rademacher and gaussian complexities: Risk bounds and structural results. *J. Mach. Learn. Res.*, 3(null):463–482, mar 2003. ISSN 1532-4435.
- Peter L Bartlett, Dylan J Foster, and Matus J Telgarsky. Spectrally-normalized margin bounds for neural networks. In I. Guyon, U. V. Luxburg, S. Bengio, H. Wallach, R. Fergus, S. Vishwanathan, and R. Garnett (eds.), *Advances in Neural Information Processing Systems*, volume 30. Curran Associates, Inc., 2017. URL <https://proceedings.neurips.cc/paper/2017/file/b22b257ad0519d4500539da3c8bcf4dd-Paper.pdf>.
- Shai Ben-David, John Blitzer, Koby Crammer, and Fernando Pereira. Analysis of representations for domain adaptation. In B. Schölkopf, J. Platt, and T. Hoffman (eds.), *Advances in Neural Information Processing Systems*, volume 19. MIT Press, 2007. URL <https://proceedings.neurips.cc/paper/2006/file/b1b0432ceafb0ce714426e9114852ac7-Paper.pdf>.
- Lucas Beyer, Xiaohua Zhai, Amélie Royer, Larisa Markeeva, Rohan Anil, and Alexander Kolesnikov. Knowledge distillation: A good teacher is patient and consistent. *CoRR*, abs/2106.05237, 2021. URL <https://arxiv.org/abs/2106.05237>.
- Tom Brown, Benjamin Mann, Nick Ryder, Melanie Subbiah, Jared D Kaplan, Prafulla Dhariwal, Arvind Neelakantan, Pranav Shyam, Girish Sastry, Amanda Askell, Sandhini Agarwal, Ariel Herbert-Voss, Gretchen Krueger, Tom Henighan, Rewon Child, Aditya Ramesh, Daniel Ziegler, Jeffrey Wu, Clemens Winter, Chris Hesse, Mark Chen, Eric Sigler, Mateusz Litwin, Scott Gray, Benjamin Chess, Jack Clark, Christopher Berner, Sam McCandlish, Alec Radford, Ilya Sutskever, and Dario Amodei. Language models are few-shot learners. In H. Larochelle, M. Ranzato, R. Hadsell, M.F. Balcan, and H. Lin (eds.), *Advances in Neural Information Processing Systems*, volume 33, pp. 1877–1901. Curran Associates, Inc., 2020. URL https://proceedings.neurips.cc/paper_files/paper/2020/file/1457c0d6bfc4967418bfb8ac142f64a-Paper.pdf.
- Peter Bühlmann. Invariance, causality and robustness, 2018.
- Mayee Chen*, Karan Goel*, Nimit Sohoni*, Fait Poms, Kayvon Fatahalian, and Christopher Re. Mandoline: Model evaluation under distribution shift. *International Conference of Machine Learning (ICML)*, 2021.
- Minshuo Chen, Haoming Jiang, Wenjing Liao, and Tuo Zhao. Nonparametric Regression on Low-Dimensional Manifolds using Deep ReLU Networks : Function Approximation and Statistical Recovery. *arXiv e-prints*, art. arXiv:1908.01842, August 2019.
- Ching-Yao Chuang, Antonio Torralba, and Stefanie Jegelka. Estimating generalization under distribution shifts via domain-invariant representations. *International conference on machine learning*, 2020.
- Ekin Dogus Cubuk, Barret Zoph, Jon Shlens, and Quoc Le. Randaugment: Practical automated data augmentation with a reduced search space. In H. Larochelle, M. Ranzato, R. Hadsell, M.F. Balcan, and H. Lin (eds.), *Advances in Neural Information Processing Systems*, volume 33, pp. 18613–18624. Curran Associates, Inc., 2020. URL <https://proceedings.neurips.cc/paper/2020/file/d85b63ef0ccb114d0a3bb7b7d808028f-Paper.pdf>.

- Luke N. Darlow, Elliot J. Crowley, Antreas Antoniou, and Amos J. Storkey. CINIC-10 is not ImageNet or CIFAR-10. *arXiv e-prints*, art. arXiv:1810.03505, October 2018.
- Jia Deng, Wei Dong, Richard Socher, Li-Jia Li, Kai Li, and Li Fei-Fei. Imagenet: A large-scale hierarchical image database. In *2009 IEEE Conference on Computer Vision and Pattern Recognition*, pp. 248–255, 2009. doi: 10.1109/CVPR.2009.5206848.
- Li Deng. The mnist database of handwritten digit images for machine learning research. *IEEE Signal Processing Magazine*, 29(6):141–142, 2012.
- Weijian Deng and Liang Zheng. Are labels always necessary for classifier accuracy evaluation? In *Proc. CVPR*, 2021.
- Weijian Deng, Stephen Gould, and Liang Zheng. What does rotation prediction tell us about classifier accuracy under varying testing environments? In *ICML*, 2021.
- Alexey Dosovitskiy, Lucas Beyer, Alexander Kolesnikov, Dirk Weissenborn, Xiaohua Zhai, Thomas Unterthiner, Mostafa Dehghani, Matthias Minderer, Georg Heigold, Sylvain Gelly, Jakob Uszkoreit, and Neil Houlsby. An image is worth 16x16 words: Transformers for image recognition at scale. In *International Conference on Learning Representations*, 2020.
- Gintare Karolina Dziugaite and Daniel M. Roy. Computing nonvacuous generalization bounds for deep (stochastic) neural networks with many more parameters than training data. In *Proceedings of the 33rd Annual Conference on Uncertainty in Artificial Intelligence (UAI)*, 2017.
- Saurabh Garg, Sivaraman Balakrishnan, Zachary C. Lipton, Behnam Neyshabur, and Hanie Sedghi. Leveraging Unlabeled Data to Predict Out-of-Distribution Performance. *arXiv e-prints*, art. arXiv:2201.04234, January 2022.
- Vikas Garg, Adam Tauman Kalai, Katrina Ligett, and Steven Wu. Learn to expect the unexpected: Probably approximately correct domain generalization. In Arindam Banerjee and Kenji Fukumizu (eds.), *Proceedings of The 24th International Conference on Artificial Intelligence and Statistics*, volume 130 of *Proceedings of Machine Learning Research*, pp. 3574–3582. PMLR, 13–15 Apr 2021. URL <https://proceedings.mlr.press/v130/garg21a.html>.
- Stanton A Glantz, Bryan K Slinker, and Torsten B Neilands. *Primer of Applied Regression and Analysis of Variance*. Health Professions Division, McGraw-Hill, New York, 1990.
- Ian Goodfellow, Jonathon Shlens, and Christian Szegedy. Explaining and harnessing adversarial examples. *arXiv 1412.6572*, 12 2014.
- Felix Gräßer, Surya Kallumadi, Hagen Malberg, and Sebastian Zaunseder. Aspect-based sentiment analysis of drug reviews applying cross-domain and cross-data learning. In *Proceedings of the 2018 International Conference on Digital Health, DH '18*, pp. 121–125, New York, NY, USA, 2018. Association for Computing Machinery. ISBN 9781450364935. doi: 10.1145/3194658.3194677. URL <https://doi.org/10.1145/3194658.3194677>.
- Keren Gu, Brandon Yang, Jiquan Ngiam, Quoc Le, and Jonathon Shlens. Using videos to evaluate image model robustness. In *SafeML Workshop at ICLR*, 2019.
- Devin Guillory, Vaishaal Shankar, Sayna Ebrahimi, Trevor Darrell, and Ludwig Schmidt. Predicting with Confidence on Unseen Distributions. In *International Conference on Computer Vision*, 2021.
- Ishaan Gulrajani and David Lopez-Paz. In Search of Lost Domain Generalization. *arXiv e-prints*, art. arXiv:2007.01434, July 2020.
- Abhishek Gupta, Alagan Anpalagan, Ling Guan, and Ahmed Shaharyar Khwaja. Deep learning for object detection and scene perception in self-driving cars: Survey, challenges, and open issues. *Array*, 10: 100057, 2021. ISSN 2590-0056. doi: <https://doi.org/10.1016/j.array.2021.100057>. URL <https://www.sciencedirect.com/science/article/pii/S2590005621000059>.

- Trygve Haavelmo. The statistical implications of a system of simultaneous equations. *Econometrica*, 11(1): 1–12, 1943. ISSN 00129682, 14680262. URL <http://www.jstor.org/stable/1905714>.
- Jeff Z. HaoChen, Colin Wei, Adrien Gaidon, and Tengyu Ma. Provable Guarantees for Self-Supervised Deep Learning with Spectral Contrastive Loss. *arXiv e-prints*, art. arXiv:2106.04156, June 2021.
- Kaiming He, Xiangyu Zhang, Shaoqing Ren, and Jian Sun. Deep Residual Learning for Image Recognition. *arXiv e-prints*, art. arXiv:1512.03385, December 2015.
- Dan Hendrycks, Xiaoyuan Liu, Eric Wallace, Adam Dziedzic, Rishabh Krishnan, and Dawn Song. Pretrained transformers improve out-of-distribution robustness. In *Proceedings of the 58th Annual Meeting of the Association for Computational Linguistics*, pp. 2744–2751, Online, July 2020a. Association for Computational Linguistics. doi: 10.18653/v1/2020.acl-main.244. URL <https://aclanthology.org/2020.acl-main.244>.
- Dan Hendrycks, Xiaoyuan Liu, Eric Wallace, Adam Dziedzic, Rishabh Krishnan, and Dawn Song. Pretrained transformers improve out-of-distribution robustness. In *Association for Computational Linguistics*, 2020b.
- Dan Hendrycks, Steven Basart, Norman Mu, Saurav Kadavath, Frank Wang, Evan Dorundo, Rahul Desai, Tyler Zhu, Samyak Parajuli, Mike Guo, Dawn Song, Jacob Steinhardt, and Justin Gilmer. The many faces of robustness: A critical analysis of out-of-distribution generalization. *ICCV*, 2021a.
- Dan Hendrycks, Kevin Zhao, Steven Basart, Jacob Steinhardt, and Dawn Song. Natural adversarial examples. *CVPR*, 2021b.
- Yiding Jiang, Dilip Krishnan, Hossein Mobahi, and Samy Bengio. Predicting the generalization gap in deep networks with margin distributions. In *International Conference on Learning Representations*, 2019. URL <https://openreview.net/forum?id=HJlQfnCqKX>.
- Yiding Jiang, Behnam Neyshabur, Hossein Mobahi, Dilip Krishnan, and Samy Bengio. Fantastic Generalization Measures and Where to Find Them. *arXiv e-prints*, art. arXiv:1912.02178, December 2019.
- Yiding Jiang, Pierre Foret, Scott Yak, Daniel M. Roy, Hossein Mobahi, Gintare Karolina Dziugaite, Samy Bengio, Suriya Gunasekar, Isabelle Guyon, and Behnam Neyshabur. NeurIPS 2020 Competition: Predicting Generalization in Deep Learning. *arXiv e-prints*, art. arXiv:2012.07976, December 2020.
- Yiding Jiang, Vaishnavh Nagarajan, Christina Baek, and J. Zico Kolter. Assessing Generalization of SGD via Disagreement. *arXiv e-prints*, art. arXiv:2106.13799, June 2021.
- M. G. Kendall. A new measure of rank correlation. *Biometrika*, 30(1/2):81–93, 1938. ISSN 00063444. URL <http://www.jstor.org/stable/2332226>.
- Nitish Shirish Keskar, Dheevatsa Mudigere, Jorge Nocedal, Mikhail Smelyanskiy, and Ping Tak Peter Tang. On large-batch training for deep learning: Generalization gap and sharp minima. *arXiv preprint arXiv:1609.04836*, 2016.
- Yoon Kim. Convolutional neural networks for sentence classification. In *Proceedings of the 2014 Conference on Empirical Methods in Natural Language Processing (EMNLP)*, 2014.
- Diederik P. Kingma and Jimmy Ba. Adam: A method for stochastic optimization, 2014. URL <http://arxiv.org/abs/1412.6980>. cite arxiv:1412.6980Comment: Published as a conference paper at the 3rd International Conference for Learning Representations, San Diego, 2015.
- Pang Wei Koh, Shiori Sagawa, Henrik Marklund, Sang Michael Xie, Marvin Zhang, Akshay Balsubramani, Weihua Hu, Michihiro Yasunaga, Richard Lanus Phillips, Irena Gao, Tony Lee, Etienne David, Ian Stavness, Wei Guo, Berton A. Earnshaw, Imran S. Haque, Sara Beery, Jure Leskovec, Anshul Kundaje, Emma Pierson, Sergey Levine, Chelsea Finn, and Percy Liang. WILDS: A benchmark of in-the-wild distribution shifts. In *International Conference on Machine Learning (ICML)*, 2021.
- Alex Krizhevsky. Learning multiple layers of features from tiny images. Technical report, 2009.

- Tengyuan Liang, Tomaso Poggio, Alexander Rakhlin, and James Stokes. Fisher-rao metric, geometry, and complexity of neural networks. In Kamalika Chaudhuri and Masashi Sugiyama (eds.), *Proceedings of the Twenty-Second International Conference on Artificial Intelligence and Statistics*, volume 89 of *Proceedings of Machine Learning Research*, pp. 888–896. PMLR, 16–18 Apr 2019. URL <https://proceedings.mlr.press/v89/liang19a.html>.
- Weixin Liang and James Zou. Metashift: A dataset of datasets for evaluating contextual distribution shifts and training conflicts. In *International Conference on Learning Representations*, 2022. URL <https://openreview.net/forum?id=MTex8qKavoS>.
- Min Lin, Qiang Chen, and Shuicheng Yan. Network In Network. *arXiv e-prints*, art. arXiv:1312.4400, December 2013.
- Yinhan Liu, Myle Ott, Naman Goyal, Jingfei Du, Mandar Joshi, Danqi Chen, Omer Levy, Mike Lewis, Luke Zettlemoyer, and Veselin Stoyanov. Roberta: A robustly optimized bert pretraining approach. *arXiv preprint arXiv:1907.11692*, 2019.
- Shangyun Lu, Bradley Nott, Aaron Olson, Alberto Todeschini, Hossein Vahabi, Yair Carmon, and Ludwig Schmidt. Harder or different? a closer look at distribution shift in dataset reproduction. In *ICML Workshop on Uncertainty and Robustness in Deep Learning*, 2020.
- Yucen Luo, Jun Zhu, Mengxi Li, Yong Ren, and Bo Zhang. Smooth neighbors on teacher graphs for semi-supervised learning. In *2018 IEEE/CVF Conference on Computer Vision and Pattern Recognition*, pp. 8896–8905, 2018. doi: 10.1109/CVPR.2018.00927.
- David A. McAllester. Pac-bayesian model averaging. In *Proceedings of the Twelfth Annual Conference on Computational Learning Theory, COLT '99*, pp. 164–170, New York, NY, USA, 1999. Association for Computing Machinery. ISBN 1581131674. doi: 10.1145/307400.307435. URL <https://doi.org/10.1145/307400.307435>.
- John Miller, Rohan Taori, Aditi Raghunathan, Shiori Sagawa, Pang Wei Koh, Vaishaal Shankar, Percy Liang, Yair Carmon, and Ludwig Schmidt. Accuracy on the line: On the strong correlation between out-of-distribution and in-distribution generalization, 2021.
- Peyman Morteza and Yixuan Li. Provable guarantees for understanding out-of-distribution detection. *Proceedings of the AAAI Conference on Artificial Intelligence*, 36(7):7831–7840, Jun. 2022. doi: 10.1609/aaai.v36i7.20752. URL <https://ojs.aaai.org/index.php/AAAI/article/view/20752>.
- Lili Mou, Rui Men, Ge Li, Yan Xu, Lu Zhang, Rui Yan, and Zhi Jin. Natural language inference by tree-based convolution and heuristic matching. In *Proceedings of the 54th Annual Meeting of the Association for Computational Linguistics (Volume 2: Short Papers)*, pp. 130–136, Berlin, Germany, August 2016. Association for Computational Linguistics. doi: 10.18653/v1/P16-2022. URL <https://aclanthology.org/P16-2022>.
- Vaishnavh Nagarajan and J Zico Kolter. Generalization in deep networks: The role of distance from initialization. In *NeurIPS Workshop on Deep Learning: Bridging Theory and Practice*, 2019.
- Ryumei Nakada and Masaaki Imaizumi. Adaptive approximation and generalization of deep neural network with intrinsic dimensionality. *Journal of Machine Learning Research*, 21(174):1–38, 2020. URL <http://jmlr.org/papers/v21/20-002.html>.
- Yuval Netzer, Tao Wang, Adam Coates, A. Bissacco, Bo Wu, and A. Ng. Reading digits in natural images with unsupervised feature learning. In *NIPS Workshop on Deep Learning and Unsupervised Feature Learning*, 2011.
- Behnam Neyshabur, Russ R Salakhutdinov, and Nati Srebro. Path-sgd: Path-normalized optimization in deep neural networks. In C. Cortes, N. Lawrence, D. Lee, M. Sugiyama, and R. Garnett (eds.), *Advances in Neural Information Processing Systems*, volume 28. Curran Associates, Inc., 2015a. URL <https://proceedings.neurips.cc/paper/2015/file/ea32c96f620053cf442ad32258076b9-Paper.pdf>.

- Behnam Neyshabur, Ryota Tomioka, and Nathan Srebro. Norm-based capacity control in neural networks. In Peter Grünwald, Elad Hazan, and Satyen Kale (eds.), *Proceedings of The 28th Conference on Learning Theory*, volume 40 of *Proceedings of Machine Learning Research*, pp. 1376–1401, Paris, France, 03–06 Jul 2015b. PMLR. URL <https://proceedings.mlr.press/v40/Neyshabur15.html>.
- Behnam Neyshabur, Srinadh Bhojanapalli, David McAllester, and Nathan Srebro. Exploring generalization in deep learning. In *Proceeding of NeurIPS*, 2017a.
- Behnam Neyshabur, Srinadh Bhojanapalli, and Nathan Srebro. A pac-bayesian approach to spectrally-normalized margin bounds for neural networks. In *International Conference on Learning Representations*, 2017b.
- Nathan Ng, Kyunghyun Cho, and Marzyeh Ghassemi. Ssmba: Self-supervised manifold based data augmentation for improving out-of-domain robustness. In *Proc. of EMNLP*, 2020.
- Jianmo Ni, Jiacheng Li, and Julian McAuley. Justifying recommendations using distantly-labeled reviews and fined-grained aspects. In *Proceedings of EMNLP*, 2019.
- Myle Ott, Sergey Edunov, Alexei Baevski, Angela Fan, Sam Gross, Nathan Ng, David Grangier, and Michael Auli. fairseq: A fast, extensible toolkit for sequence modeling. In *Proceedings of NAACL-HLT 2019: Demonstrations*, 2019.
- Nicolas Papernot, Patrick McDaniel, Ian Goodfellow, Somesh Jha, Z. Berkay Celik, and Ananthram Swami. Practical black-box attacks against machine learning. In *Proceedings of the 2017 ACM on Asia Conference on Computer and Communications Security, ASIA CCS '17*, pp. 506–519, New York, NY, USA, 2017. Association for Computing Machinery. ISBN 9781450349444. doi: 10.1145/3052973.3053009. URL <https://doi.org/10.1145/3052973.3053009>.
- Gabriel Pereyra, George Tucker, Jan Chorowski, Łukasz Kaiser, and Geoffrey Hinton. Regularizing neural networks by penalizing confident output distributions. In *ICLR*, 2017.
- Jonas Peters, Peter Bühlmann, and Nicolai Meinshausen. Causal inference using invariant prediction: identification and confidence intervals, 2015.
- Alec Radford, Jong Wook Kim, Chris Hallacy, Aditya Ramesh, Gabriel Goh, Sandhini Agarwal, Girish Sastry, Amanda Askell, Pamela Mishkin, Jack Clark, Gretchen Krueger, and Ilya Sutskever. Learning transferable visual models from natural language supervision. *CoRR*, abs/2103.00020, 2021. URL <https://arxiv.org/abs/2103.00020>.
- Benjamin Recht, Rebecca Roelofs, Ludwig Schmidt, and Vaishaal Shankar. Do cifar-10 classifiers generalize to cifar-10? 2018. <https://arxiv.org/abs/1806.00451>.
- Benjamin Recht, Rebecca Roelofs, Ludwig Schmidt, and Vaishaal Shankar. Do ImageNet classifiers generalize to ImageNet? In Kamalika Chaudhuri and Ruslan Salakhutdinov (eds.), *Proceedings of the 36th International Conference on Machine Learning*, volume 97 of *Proceedings of Machine Learning Research*, pp. 5389–5400. PMLR, 09–15 Jun 2019. URL <https://proceedings.mlr.press/v97/recht19a.html>.
- Alexandra Birch Rico Sennrich, Barry Haddow. Improving neural machine translation models with monolingual data. In *Proc. of ACL*, 2016.
- Salah Rifai, Yann N Dauphin, Pascal Vincent, Yoshua Bengio, and Xavier Muller. The manifold tangent classifier. In J. Shawe-Taylor, R. Zemel, P. Bartlett, F. Pereira, and K.Q. Weinberger (eds.), *Advances in Neural Information Processing Systems*, volume 24. Curran Associates, Inc., 2011. URL <https://proceedings.neurips.cc/paper/2011/file/d1f44e2f09dc172978a4d3151d11d63e-Paper.pdf>.
- Alexey Romanov and Chaitanya Shivade. Lessons from natural language inference in the clinical domain. 2018. URL <http://arxiv.org/abs/1808.06752>.

- Olga Russakovsky, Jia Deng, Hao Su, Jonathan Krause, Sanjeev Satheesh, Sean Ma, Zhiheng Huang, Andrej Karpathy, Aditya Khosla, Michael Bernstein, Alexander C. Berg, and Li Fei-Fei. Imagenet large scale visual recognition challenge. *International Journal of Computer Vision*, 115(3):211–252, Dec 2015. ISSN 1573-1405. doi: 10.1007/s11263-015-0816-y. URL <https://doi.org/10.1007/s11263-015-0816-y>.
- Akiyoshi Sannai, Masaaki Imaizumi, and Makoto Kawano. Improved generalization bounds of group invariant equivariant deep networks via quotient feature spaces. In *Conference on Uncertainty in Artificial Intelligence*, 2021.
- Yair Schiff, Brian Quanz, Payel Das, and Pin-Yu Chen. Predicting deep neural network generalization with perturbation response curves. In *Neural Information Processing Systems*, 2021.
- Johannes Schmidt-Hieber. Deep ReLU network approximation of functions on a manifold. *arXiv e-prints*, art. arXiv:1908.00695, August 2019.
- Karen Simonyan and Andrew Zisserman. Very deep convolutional networks for large-scale image recognition. In *Proceedings of the International Conference on Learning Representations*, 2015.
- Jure Sokolić, Raja Giryes, Guillermo Sapiro, and Miguel R. D. Rodrigues. Generalization error of deep neural networks: Role of classification margin and data structure. In *2017 International Conference on Sampling Theory and Applications (SampTA)*, pp. 147–151, 2017. doi: 10.1109/SAMP.2017.8024476.
- Taiji Suzuki. Adaptivity of deep relu network for learning in besov and mixed smooth besov spaces: optimal rate and curse of dimensionality. In *International Conference on Learning Representations*, 2018.
- Taiji Suzuki and Atsushi Nitanda. Deep learning is adaptive to intrinsic dimensionality of model smoothness in anisotropic besov space. In M. Ranzato, A. Beygelzimer, Y. Dauphin, P.S. Liang, and J. Wortman Vaughan (eds.), *Advances in Neural Information Processing Systems*, volume 34, pp. 3609–3621. Curran Associates, Inc., 2021. URL <https://proceedings.neurips.cc/paper/2021/file/1dacb10f0623c67cb7dbb37587d8b38a-Paper.pdf>.
- Mingxing Tan and Quoc Le. EfficientNet: Rethinking model scaling for convolutional neural networks. In Kamalika Chaudhuri and Ruslan Salakhutdinov (eds.), *Proceedings of the 36th International Conference on Machine Learning*, volume 97 of *Proceedings of Machine Learning Research*, pp. 6105–6114. PMLR, 09–15 Jun 2019. URL <https://proceedings.mlr.press/v97/tan19a.html>.
- Rohan Taori, Achal Dave, Vaishal Shankar, Nicholas Carlini, Benjamin Recht, and Ludwig Schmidt. Measuring robustness to natural distribution shifts in image classification. In H. Larochelle, M. Ranzato, R. Hadsell, M.F. Balcan, and H. Lin (eds.), *Advances in Neural Information Processing Systems*, volume 33, pp. 18583–18599. Curran Associates, Inc., 2020. URL <https://proceedings.neurips.cc/paper/2020/file/d8330f857a17c53d217014ee776bfd50-Paper.pdf>.
- V. N. Vapnik and A. Ya. Chervonenkis. On the uniform convergence of relative frequencies of events to their probabilities. *Theory of Probability & Its Applications*, 16(2):264–280, 1971. doi: 10.1137/1116025. URL <https://doi.org/10.1137/1116025>.
- Ramakrishna Vedantam, David Lopez-Paz, and David J. Schwab. An empirical investigation of domain generalization with empirical risk minimizers. In *Neural Information Processing Systems*, 2021.
- Vikas Verma, Alex Lamb, Christopher Beckham, Amir Najafi, Ioannis Mitliagkas, David Lopez-Paz, and Yoshua Bengio. Manifold mixup: Better representations by interpolating hidden states. In Kamalika Chaudhuri and Ruslan Salakhutdinov (eds.), *Proceedings of the 36th International Conference on Machine Learning*, volume 97 of *Proceedings of Machine Learning Research*, pp. 6438–6447. PMLR, 09–15 Jun 2019. URL <https://proceedings.mlr.press/v97/verma19a.html>.
- Haohan Wang, Songwei Ge, Zachary Lipton, and Eric P Xing. Learning robust global representations by penalizing local predictive power. In H. Wallach, H. Larochelle, A. Beygelzimer, F. d'Alché-Buc, E. Fox, and R. Garnett (eds.), *Advances in Neural Information Processing Systems*, volume 32. Curran Associates, Inc., 2019. URL https://proceedings.neurips.cc/paper_files/paper/2019/file/3eefceb8087e964f89c2d59e8a249915-Paper.pdf.

- Jason Wei and Kai Zou. EDA: Easy data augmentation techniques for boosting performance on text classification tasks. In *Proceedings of the 2019 Conference on Empirical Methods in Natural Language Processing and the 9th International Joint Conference on Natural Language Processing (EMNLP-IJCNLP)*, pp. 6383–6389, Hong Kong, China, November 2019. Association for Computational Linguistics. URL <https://www.aclweb.org/anthology/D19-1670>.
- J. Wiens, S. Saria, M. Sendak, M. Ghassemi, V. Liu, F. Doshi-Velez, K. Jung, K. Heller, D. Kale, M. Saeed, P. Ossorio, S. Thadaneys-Israni, and A. Goldenberg. Do no harm: A roadmap for responsible machine learning for healthcare. *Nature Medicine*, 25(10):1337–1340, 2019.
- Adina Williams, Nikita Nangia, and Samuel Bowman. A broad-coverage challenge corpus for sentence understanding through inference. In *Proceedings of the 2018 Conference of the North American Chapter of the Association for Computational Linguistics: Human Language Technologies, Volume 1 (Long Papers)*, pp. 1112–1122. Association for Computational Linguistics, 2018. URL <http://aclweb.org/anthology/N18-1101>.
- Mitchell Wortsman, Gabriel Ilharco, Jong Wook Kim, Mike Li, Simon Kornblith, Rebecca Roelofs, Raphael Gontijo Lopes, Hannaneh Hajishirzi, Ali Farhadi, Hongseok Namkoong, and Ludwig Schmidt. Robust fine-tuning of zero-shot models. In *Proceedings of the IEEE/CVF Conference on Computer Vision and Pattern Recognition (CVPR)*, pp. 7959–7971, June 2022.
- Lingxi Xie, Jingdong Wang, Zhen Wei, Meng Wang, and Qi Tian. DisturbLabel: Regularizing CNN on the Loss Layer. *arXiv e-prints*, art. arXiv:1605.00055, April 2016.
- Qizhe Xie, Zihang Dai, Eduard Hovy, Minh-Thang Luong, and Quoc V Le. Unsupervised data augmentation for consistency training. *arXiv preprint arXiv:1904.12848*, 2019.
- Saining Xie, Ross Girshick, Piotr Dollár, Zhuowen Tu, and Kaiming He. Aggregated residual transformations for deep neural networks. *arXiv preprint arXiv:1611.05431*, 2016.
- Yuichi Yoshida and Takeru Miyato. Spectral Norm Regularization for Improving the Generalizability of Deep Learning. *arXiv e-prints*, art. arXiv:1705.10941, May 2017.
- Chiyuan Zhang, Samy Bengio, Moritz Hardt, Benjamin Recht, and Oriol Vinyals. Understanding deep learning requires rethinking generalization. *arXiv e-prints*, art. arXiv:1611.03530, November 2016.
- Hongyi Zhang, Moustapha Cisse, Yann N. Dauphin, and David Lopez-Paz. mixup: Beyond empirical risk minimization. In *International Conference on Learning Representations*, 2018. URL <https://openreview.net/forum?id=r1Ddp1-Rb>.
- Yuchen Zhang, Tianle Liu, Mingsheng Long, and Michael Jordan. Bridging theory and algorithm for domain adaptation. In Kamalika Chaudhuri and Ruslan Salakhutdinov (eds.), *Proceedings of the 36th International Conference on Machine Learning*, volume 97 of *Proceedings of Machine Learning Research*, pp. 7404–7413. PMLR, 09–15 Jun 2019. URL <https://proceedings.mlr.press/v97/zhang19i.html>.
- Zhun Zhong, Liang Zheng, Guoliang Kang, Shaozi Li, and Yi Yang. Random erasing data augmentation. *Proceedings of the AAAI Conference on Artificial Intelligence*, 34(07):13001–13008, Apr. 2020. doi: 10.1609/aaai.v34i07.7000. URL <https://ojs.aaai.org/index.php/AAAI/article/view/7000>.
- Sicheng Zhu, Bang An, and Furong Huang. Understanding the generalization benefit of model invariance from a data perspective. In *NeurIPS*, 2021.

A Experimental Setup

In this section we present full details of our experimental setup, including data preprocessing and specifics on model architecture and hyperparameter space. All models are trained on a single RTX6000 GPU.

A.1 Data Preprocessing

Large ImageNet scale datasets are preprocessed using the pipeline provided by Taori et al. (2020). Small scale image classification datasets are preprocessed by normalizing pixel values and resizing to 32×32 if necessary. We use the same preprocessing steps for sentiment analysis and NLI experiments. All data is first tokenized using a GPT-2 style tokenizer and BPE vocabulary provided by fairseq (Ott et al., 2019). This BPE vocabulary consists of 50263 types. Corresponding labels are encoded using a label dictionary consisting of as many types as there are classes. Input text and labels are then binarized for model training.

A.2 Model Architecture

The full list of the 196 models we evaluate from the Imagenet-Testbed (Taori et al., 2020) is provided below:

```
alexnet_lpf2, vit_large_patch32_384, wide_resnet101_2, resnet50_aws_baseline, resnet50_feature_cutmix, densenet169,
efficientnet-b2-autoaug, vgg11_bn, resnet50_with_jpeg_compression_aws, BiT-M-R101x3-nonfinetuned, efficientnet-b6-autoaug,
resnet18_lpf5, mobilenet_v2, resnet50_swsl, densenet121_lpf3, BiT-M-R101x1-nonfinetuned, efficientnet-b2-advprop-autoaug,
resnext101_32x8d_swsl, resnet50_with_fog_aws, resnet50_trained_on_SIN_and_IN, resnext101_32x4d, resnet50_with_
contrast_aws, FixResNet50CutMix, resnet50_imagenet_subsample_1_of_32_batch64_original_images, resnext101_32x4d_
swsl, squeezeNet1_1, resnet50_imagenet_subsample_1_of_16_batch64_original_images, resnet18-rotation-nocrop_40,
resnet101_cutmix, efficientnet-b3, resnet50_with_motion_blur_aws, vit_large_patch16_384, efficientnet-b4, resnet50_
lpf3, dpn107, resnext101_32x8d_deepaugmt_augmix, vgg19, resnet18_ssl, vgg13_bn, vgg13, resnet50_with_pixelate_aws,
senet154, resnet18_lpf2, shufflenet_v2_x1_0, se_resnet101, alexnet_lpf5, densenet121, efficientnet-b3-advprop-autoaug,
resnet50_augmix, resnet50_simsiam, efficientnet-b0-advprop-autoaug, resnet50_imagenet_subsample_500_classes_batch64_
original_images, vgg16_lpf2, mnasnet1_0, resnet34_lpf2, dpn68b, mobilenet_v2_lpf3, resnet101_lpf3, alexnet, vgg16_bn,
efficientnet-b0, inceptionv3, resnet18-rotation-worst10_30, resnet152_3x_simclr_v2_finetuned_100pct_tf_port, resnet50_
imagenet_subsample_1_of_2_batch64_original_images, wide_resnet50_2, polynet, efficientnet-b7-randaug, dpn131, vgg16_
bn_lpf2, instagram-resnext101_32x16d, vgg16_bn_lpf5, resnet50_linf_eps8_robust, efficientnet-b1-advprop-autoaug,
inceptionv4, vit_b_32_clip_zeroshot, resnet18-rotation-worst10_40, resnet50_imagenet_100percent_batch64_original_
images, resnet50_with_frost_aws, efficientnet-b3-autoaug, resnet50_imagenet_subsample_125_classes_batch64_original_
images, efficientnet-b7-autoaug, resnet50_ssl, vgg16_lpf5, vit_base_patch16_224, resnet34_lpf5, resnet152, resnext50_
32x4d, FixPNASNet, resnet50_with_saturate_aws, FixResNet50CutMix_v2, densenet121_lpf5, resnet50_imagenet_subsample_1_of_
4_batch64_original_images, resnet18-rotation-random_40, resnet50_adv_train_free, resnet18_lpf3, BiT-M-R50x3-nonfinetuned,
efficientnet-b7-advprop-autoaug, resnet50_with_spatter_aws, resnet50_trained_on_SIN, resnet50_simclr_v2_finetuned_100pct_tf_
port, pnasnet5large, BiT-M-R50x3-ILSVRC2012, resnet50_imagenet_subsample_250_classes_batch64_original_images, efficientnet-b5,
resnet50_deepaugmt, efficientnet-b5-randaug, resnet50_lpf2, se_resnext50_32x4d, resnet50_clip_zeroshot, resnext50_32x4d_
swsl, BiT-M-R50x1-nonfinetuned, BiT-M-R101x3-ILSVRC2012, resnet50_imagenet_subsample_1_of_8_batch64_original_images, vit_
large_patch16_224, efficientnet-b1-autoaug, efficientnet-b6-advprop-autoaug, efficientnet-b5-autoaug, resnet50_with_zoom_
blur_aws, resnext50_32x4d_ssl, FixResNet50_v2, resnet50_lpf5, resnet101, resnet18_swsl, efficientnet-b2, squeezeNet1_0,
resnet152-imagenet11k, resnet50_simclr_v2_linear_probe_tf_port, alexnet_lpf3, bninception, efficientnet-b8-advprop-autoaug,
resnet50_linf_eps4_robust, FixResNet50, mnasnet0_5, resnet50_mixup, densenet121_lpf2, resnet18-rotation-standard_40, se_
resnext101_32x4d, resnet18-rotation-random_30, efficientnet-b0-autoaug, efficientnet-b4-autoaug, vgg11, resnext101_32x8d,
BiT-M-R50x1-ILSVRC2012, resnet50, resnet50_with_gaussian_noise_contrast_motion_blur_jpeg_compression_aws, shufflenet_v2_x0_5,
dpn92, xception, resnet152_3x_simclr_v2_linear_probe_tf_port, dpn98, bninception-imagenet21k, efficientnet-b5-advprop-autoaug,
resnext101_32x16d_ssl, vit_base_patch32_384, densenet201, inceptionresnetv2, cafferesnet101, instagram-resnext101_32x8d,
resnet34, FixResNet50_no_adaptation, resnext101_32x8d_ssl, resnet101_lpf5, resnet101_lpf3, bninception, efficientnet-b8-advprop-autoaug,
nasnetamobile, mobilenet_v2_lpf2, resnet101_lpf2, se_resnet50, dpn68, resnet50_with_brightness_aws, resnext101_64x4d,
resnext101_32x4d_ssl, vgg19_bn, fbresnet152, resnet50_deepaugmt_augmix, se_resnet152, resnet50_cutout, resnet50_cutmix,
resnet50_l2_eps3_robust, efficientnet-b1, resnet50_with_defocus_blur_aws, BiT-M-R101x1-ILSVRC2012, vgg16_bn_lpf3, resnet50_
trained_on_SIN_and_IN_then_finetuned_on_IN, nasnetalarge, resnet50_with_gaussian_noise_aws, vit_base_patch16_384, resnet50_
swav, resnet50_with_greyscale_aws, vgg16, resnet34_lpf3, efficientnet-b4-advprop-autoaug, vgg16_lpf3, resnet18, densenet161
```

Our small image classification models are Network in Network (NiN) (Lin et al., 2013), VGG (Simonyan & Zisserman, 2015), and CNN models. Training and hyperparameter details for these models are provided in Jiang et al. (2020).

For natural language tasks, our CNN models are based on the architecture in Kim (2014). Our input embeddings are 512 dimensional, which we treat as our channel dimension. Our base model applies a set of three one dimensional convolutions of kernel size 3, 4, and 5 with 256 output channels. We modulate the number of stacked convolutions (depth) as well as the channel size (width). Each convolution generates a separate representation that is max pooled across the sequence and concatenated together. We feed this representation into a MLP classifier with a single hidden layer of 512 dimensions. We apply dropout of 0.2 to our inputs and MLP classifier.

Our RoBERTa models use a pre-trained RoBERTa_{BASE} model provided by fairseq. Classification token embeddings are fed into an MLP classifier with a single hidden layer of 512 dimensions. All models are written within the fairseq framework (Ott et al., 2019) and trained on a single RTX6000 or T4 GPU.

Hyperparameter	CNN		RoBERTa	
	SA	NLI	SA	NLI
Batch Size	{32, 64, 128}	{32, 64, 128 }	{8, 16, 32}	{8, 16, 32}
Depth	{1, 2, 3 }	{1, 2, 3 }	1	1
Width	{128, 256, 512}	{128, 256, 512 }	768	768
Dropout	{0.0, 0.25, 0.5}	{0.0, 0.25}	{0.0, 0.1}	{0.0, 0.1}
Weight Decay	{0.0, 0.0001, 0.0005}	0.0	{0.0, 0.0001, 0.0005}	{0.0, 0.0001, 0.0005}
Label Noise	0.0	{0.0, 0.2, 0.4}	{0.0, 0.2, 0.4}	{0.0, 0.2, 0.4}

Table 6: Possible hyperparameter values for each architecture and task.

A.3 Model Hyperparameters

Hyperparameter values for image classification models are provided in Jiang et al. (2020). For natural language models we vary the following hyperparameters: training domain, batch size, depth, width, dropout, weight decay, and label noise. For training domains, on sentiment analysis we choose between `books`, `clothing`, `home`, `kindle`, `movies`, `pets`, `sports`, `tech`, `tools`, `toys`. For training domains on NLI, we choose between `slate`, `government`, `fiction`, `telephone`, `travel`. NLI datasets include additional test sets `oup`, `nineeleven`, `facetoface`, `verbatim`, `letters`. Possible values for all other hyperparameters are provided in Table 6

A.4 Model Training

All models are trained with the Adam optimizer (Kingma & Ba, 2014) with $\beta = (0.9, 0.98)$ and $\epsilon = 1 \times 10^{-6}$. CNN models are trained with learning rate 1×10^{-3} and RoBERTa models are trained with learning rate 1×10^{-5} . We use an inverse square root learning rate scheduler to anneal learning rate over training. We early stop CNN models on sentiment analysis at 0.04 cross entropy and on NLI at 0.03 cross entropy. We early stop RoBERTa models on sentiment analysis at 0.05 cross entropy and on NLI at 0.03 cross entropy. Training details for image classification models are provided in Jiang et al. (2020).

A.5 Transformation Magnitudes

We define how to determine the magnitude of each data transformation below, and use a maximum value based on best practices provided in their respective papers.

- **RandAugment:** The magnitude of a transformation is determined by the magnitude parameter in the RandAugment algorithm as well as the number of augmentations applied. In our experiments we consider transformations with a maximum magnitude of 15, with 3 augmentations for larger ImageNet models and 1 augmentation for smaller models.
- **Translate:** The magnitude of a transformation is determined by the maximum percentage of the image the image will be translated in both the X- and Y-axes. In our experiments we consider translations of up to 10% of the size of the image in both axes.
- **Erase:** The magnitude of the erase transformation is determined by the percentage of the image erased. In our experiments we consider transformations that remove a maximum size of 33% of the total image area and an aspect ratio between 1/3 and 10/3.
- **Flip and Crop:** The magnitude of the flip and crop transformation is determined by the flip probability and the crop size. In our experiments we consider transformations that flip the image 50% of the time and crop the image with a lower bound of 8% of total image area and an aspect ratio between 3/4 and 4/3. Images are resized to 32×32 after cropping.
- **SSMBA:** The magnitude of a SSMBA transformation is determined by the percentage of tokens corrupted, where of the tokens selected, 10% are unmasked, 10% are randomly replaced, and the

remaining 80% are masked. In our experiments we consider SSMBAs with a maximum of 15% of tokens corrupted.

- **EDA:** The magnitude of an EDA transformation is determined by the percentage of tokens noised. In our experiments we consider transformations with a maximum of 10% of the tokens.
- **Backtranslation:** The magnitude of a backtranslation operation is determined by the temperature of the softmax-ed distribution from which we sample tokens. In our experiments we consider transformations with a maximum temperature of 0.7.
- **Random Replacement:** The magnitude of a random replacement operation is determined by the percentage of tokens replaced. In our experiments we consider transformations with a maximum of 15% of tokens replaced.

B Additional Experiments

B.1 Norm-Based Complexity Measures

Following (Jiang et al., 2019), we calculate our spectral norm measure as $\prod_{i=1}^d \|\mathbf{W}_i\|_2^2$ and Frobenius norm measure $\prod_{i=1}^d \|\mathbf{W}_i\|_F^2$. We do not list results on these measures as the correlations are often negative or 0.

B.2 Cross-Domain Correlation

In this set of experiments we measure the correlation between neighborhood invariance and generalization values of a single model trained on a single training domain evaluated across different OOD test domains. For natural language experiments we average correlations across all CNN and RoBERTa models and training domains and call these the **CNN** τ and **Roberta** τ . Since these results are rank correlations over only 9 values, they are quite noisy. Results are presented in Table 7.

Neighborhood invariance performs quite poorly on both models, although they still outperform ATC baselines. We hypothesize different regions of the input space may have different optimal levels of smoothness that achieve the lowest generalization error. Our value of interest is then not the absolute smoothness, but the *relative* smoothness compared to this optimal value. These values are the same when comparing different models evaluated on the same domain, but are not the same for the same model evaluated on different domains, making correlating across domains difficult. On the natural image manifold where domains are more well behaved and uniform compared to the natural language manifold, the relative smoothness may not differ much between domains allowing us to correlate our measure across domains.

B.3 Negative Entropy Results

As an alternative to defining the invariance as the maximum value of the neighborhood decision distribution in Eq. 1, we also consider defining it using the negative entropy of the same distribution:

$$\mu(f, x) = \sum_{j \in \mathcal{Y}} p_j(x) \log p_j(x)$$

A full table of results including metrics calculated on neighborhood invariance measured with negative entropy is provided in Table 8. We refer to measures calculated with entropy as **NE-SSMBA**, **NE-EDA**, **NE-BT**, and **NE-Random**. For most metrics, NE-* methods perform similarly or slightly worse.

C Full Results

We provide a full breakdown of results on the correlation metrics R^2 (Tables 10, 11, 12, 13, 14, 15), macro τ (Tables 17, 18, 19, 20, 21, 22), micro τ (Tables 23, 24), and ID τ (Tables 25, 26, 27) for each set of datasets and models. We also provide additional standard deviations for all main results in Table 2.

Task	Measure	CNN τ	RoBERTa τ
SA	NI-SSMBA	0.360	0.010
	NI-EDA	0.431	0.266
	NI-BT	0.505	0.245
	NI-RandRep	0.570	0.150
	ATC-NE	0.543	0.228
	ATC-MC	0.539	0.224
NLI	NI-SSMBA	0.022	0.260
	NI-EDA	0.102	0.335
	NI-BT	0.089	0.333
	NI-RandRep	0.226	0.440
	ATC-NE	0.219	0.231
	ATC-MC	0.223	0.239

Table 7: Correlation metrics evaluating the ability of our smoothness measure to predict OOD generalization across test datasets. Our smoothness measures achieves strong correlation in image classification tasks but fails in natural language tasks.

Task	Measure	CNN				RoBERTa				
		R^2	MAE	Macro τ	Micro τ	R^2	MAE	Macro τ	Micro τ	
SA	NI-SSMBA	0.662	1.93	0.677	0.689	0.972	1.29	0.832	0.829	
	NI-EDA	0.641	2.04	0.664	0.649	0.968	1.45	0.830	0.810	
	NI-BT	0.550	2.99	0.592	0.501	0.961	1.47	0.813	0.801	
	NI-RandRep	0.409	2.64	0.544	0.554	0.967	1.27	0.821	0.816	
	NE-SSMBA	0.595	2.53	0.708	0.713	0.971	1.32	0.830	0.824	
	NE-EDA	0.534	2.71	0.698	0.674	0.965	1.55	0.825	0.801	
	NE-BT	0.471	3.59	0.618	0.541	0.961	1.46	0.813	0.799	
	NE-RandRep	0.283	3.37	0.570	0.552	0.964	1.34	0.818	0.809	
	ATC-NE	0.530	3.80	0.506	0.642	0.849	3.59	0.684	0.706	
	ATC-MC	0.528	3.76	0.507	0.642	0.863	3.54	0.698	0.716	
	NLI	NI-SSMBA	0.575	2.09	0.570	0.534	0.933	1.19	0.750	0.730
		NI-EDA	0.577	2.04	0.581	0.511	0.941	1.26	0.789	0.757
		NI-BT	0.509	2.11	0.470	0.449	0.944	1.07	0.759	0.740
		NI-RandRep	0.451	2.20	0.452	0.428	0.890	1.70	0.688	0.647
NE-SSMBA		0.588	2.20	0.579	0.520	0.941	1.39	0.738	0.711	
NE-EDA		0.606	2.11	0.597	0.512	0.937	1.48	0.767	0.732	
NE-BT		0.536	2.27	0.480	0.422	0.954	1.12	0.764	0.750	
NE-RandRep		0.457	2.36	0.451	0.397	0.904	1.79	0.665	0.591	
ATC-NE		0.378	3.57	0.430	0.294	0.673	2.35	0.536	0.52	
ATC-MC		0.382	3.57	0.433	0.297	0.718	2.21	0.570	0.556	

Table 8: Correlation metrics evaluating the quality of our neighborhood invariance measure on two tasks, sentiment analysis and natural language inference, and two architectures, CNN and RoBERTa. Details on metric calculations and baselines are provided in sections 4.3 and 4.5. This full table of results includes metrics calculated with neighborhood negative entropy measure as well.

Measure	Test Domain						
	ImageNetV2	ImageNet-Sketch	ObjectNet	ImageNet-Vid	YTBB	ImageNet-R	ImageNet-A
NI-RandAug	0.810	0.641	0.613	0.767	0.570	0.763	0.577
NI-Translate	0.794	0.436	0.461	0.642	0.395	0.560	0.468
NI-Erase	0.715	0.222	0.384	0.635	0.399	0.398	0.446
NI-FC	0.767	0.406	0.516	0.706	0.446	0.618	0.679
ATC-MC	0.980	0.710	0.451	0.552	0.200	0.463	0.159
ATC-NE	0.991	0.709	0.392	0.484	0.229	0.441	0.209

Table 9: Full R^2 metrics for all ImageNet test domains. We average values across models.

Model	Train Domain	Measure	Test Domain		
			SVHN	Colored MNIST	MNIST
NiN	SVHN	NI-RandAug	—	0.785	0.744
		NI-Translate	—	0.728	0.642
		NI-Erase	—	0.088	0.218
		NI-FC	—	0.134	0.283
		ATC-NE	—	0.506	0.725
		ATC-MC	—	0.615	0.769

Table 10: Full R^2 metrics for all test domains for image classification models on SVHN, Colored MNIST, and MNIST.

Model	Train Domain	Measure	Test Domain			
			CIFAR10	CINIC10	CIFAR10.1	CIFAR10.2
NiN	CIFAR10	NI-RandAug	—	0.898	0.927	0.876
		NI-Translate	—	0.688	0.864	0.730
		NI-Erase	—	0.404	0.526	0.547
		NI-FC	—	0.109	0.028	0.000
		ATC-NE	—	0.237	0.575	0.435
		ATC-MC	—	0.252	0.538	0.390
ResNet	CIFAR10	NI-RandAug	—	0.816	0.844	0.853
		NI-Translate	—	0.889	0.899	0.836
		NI-Erase	—	0.807	0.812	0.783
		NI-FC	—	0.726	0.628	0.660
		ATC-NE	—	0.736	0.782	0.693
		ATC-MC	—	0.702	0.760	0.680
VGG	CIFAR10	NI-RandAug	—	0.969	0.950	0.929
		NI-Translate	—	0.849	0.844	0.809
		NI-Erase	—	0.096	0.100	0.104
		NI-FC	—	0.637	0.524	0.487
		ATC-NE	—	0.557	0.774	0.724
		ATC-MC	—	0.559	0.764	0.709
CNN	CINIC10	NI-RandAug	0.922	—	0.876	0.865
		NI-Translate	0.516	—	0.449	0.407
		NI-Erase	0.603	—	0.504	0.548
		NI-FC	0.416	—	0.397	0.395
		ATC-NE	0.869	—	0.750	0.724
		ATC-MC	0.868	—	0.741	0.716

Table 11: Full R^2 metrics for all test domains for image classification models on CIFAR10, CINIC10, CIFAR10.1, and CIFAR10.2.

Train Domain	Measure	Test Domain									
		books	clothing	home	kindle	movies	pets	sports	tech	tools	toys
books	NI-SSMBA	—	0.688	0.771	0.752	0.683	0.823	0.762	0.697	0.711	0.729
	NI-EDA	—	0.720	0.725	0.699	0.689	0.810	0.693	0.663	0.727	0.805
	NI-BT	—	0.560	0.663	0.639	0.593	0.675	0.602	0.591	0.592	0.658
	NI-RandRep	—	0.413	0.418	0.331	0.343	0.479	0.373	0.304	0.401	0.496
	ATC-NE	—	0.765	0.859	0.828	0.777	0.834	0.834	0.791	0.814	0.872
	ATC-MC	—	0.759	0.854	0.821	0.771	0.828	0.830	0.790	0.808	0.871
clothing	NI-SSMBA	0.517	—	0.601	0.531	0.525	0.535	0.566	0.484	0.549	0.631
	NI-EDA	0.409	—	0.419	0.452	0.408	0.395	0.457	0.388	0.486	0.534
	NI-BT	0.234	—	0.164	0.267	0.273	0.121	0.191	0.164	0.193	0.355
	NI-RandRep	0.236	—	0.237	0.223	0.250	0.212	0.213	0.156	0.246	0.335
	ATC-NE	0.480	—	0.673	0.478	0.467	0.466	0.739	0.299	0.772	0.847
	ATC-MC	0.477	—	0.675	0.477	0.466	0.474	0.742	0.300	0.772	0.848
home	NI-SSMBA	0.533	0.545	—	0.524	0.511	0.665	0.648	0.576	0.604	0.592
	NI-EDA	0.412	0.554	—	0.451	0.433	0.586	0.496	0.417	0.525	0.657
	NI-BT	0.313	0.260	—	0.327	0.316	0.346	0.366	0.304	0.385	0.408
	NI-RandRep	0.273	0.260	—	0.236	0.325	0.286	0.299	0.270	0.282	0.370
	ATC-NE	0.608	0.861	—	0.675	0.618	0.838	0.838	0.720	0.863	0.894
	ATC-MC	0.612	0.861	—	0.679	0.626	0.838	0.839	0.719	0.863	0.895
kindle	NI-SSMBA	0.645	0.680	0.650	—	0.626	0.765	0.659	0.551	0.556	0.634
	NI-EDA	0.722	0.688	0.695	—	0.662	0.785	0.690	0.658	0.623	0.783
	NI-BT	0.655	0.674	0.684	—	0.625	0.745	0.704	0.695	0.649	0.735
	NI-RandRep	0.325	0.364	0.253	—	0.269	0.442	0.292	0.244	0.274	0.445
	ATC-NE	0.747	0.659	0.701	—	0.690	0.792	0.717	0.505	0.610	0.776
	ATC-MC	0.759	0.642	0.699	—	0.687	0.784	0.708	0.507	0.594	0.765
movies	NI-SSMBA	0.541	0.640	0.658	0.615	—	0.633	0.656	0.583	0.653	0.741
	NI-EDA	0.542	0.662	0.571	0.676	—	0.629	0.594	0.574	0.636	0.789
	NI-BT	0.602	0.679	0.677	0.653	—	0.723	0.739	0.700	0.709	0.754
	NI-RandRep	0.194	0.276	0.281	0.279	—	0.228	0.316	0.216	0.316	0.369
	ATC-NE	0.698	0.719	0.708	0.668	—	0.718	0.707	0.611	0.752	0.818
	ATC-MC	0.707	0.725	0.713	0.664	—	0.732	0.711	0.624	0.755	0.820
pets	NI-SSMBA	0.458	0.543	0.578	0.529	0.548	—	0.606	0.528	0.590	0.721
	NI-EDA	0.426	0.552	0.554	0.467	0.513	—	0.546	0.463	0.549	0.677
	NI-BT	0.485	0.523	0.477	0.549	0.563	—	0.581	0.550	0.580	0.587
	NI-RandRep	0.260	0.333	0.284	0.302	0.320	—	0.304	0.271	0.345	0.432
	ATC-NE	0.641	0.851	0.849	0.651	0.680	—	0.825	0.591	0.812	0.883
	ATC-MC	0.644	0.846	0.848	0.648	0.683	—	0.824	0.589	0.810	0.883
sports	NI-SSMBA	0.499	0.530	0.569	0.524	0.463	0.573	—	0.517	0.590	0.721
	NI-EDA	0.464	0.514	0.460	0.489	0.381	0.508	—	0.448	0.541	0.594
	NI-BT	0.406	0.295	0.334	0.383	0.381	0.325	—	0.331	0.393	0.411
	NI-RandRep	0.283	0.173	0.212	0.256	0.219	0.239	—	0.204	0.231	0.331
	ATC-NE	0.712	0.900	0.926	0.744	0.656	0.891	—	0.828	0.931	0.953
	ATC-MC	0.723	0.897	0.926	0.754	0.665	0.896	—	0.833	0.933	0.952
tech	NI-SSMBA	0.610	0.508	0.635	0.620	0.596	0.604	0.636	—	0.545	0.848
	NI-EDA	0.550	0.475	0.519	0.603	0.608	0.581	0.587	—	0.532	0.649
	NI-BT	0.588	0.447	0.572	0.632	0.597	0.558	0.603	—	0.523	0.648
	NI-RandRep	0.340	0.241	0.262	0.307	0.337	0.285	0.291	—	0.200	0.432
	ATC-NE	0.766	0.820	0.904	0.791	0.817	0.866	0.874	—	0.882	0.893
	ATC-MC	0.771	0.823	0.904	0.794	0.817	0.864	0.875	—	0.882	0.893
tools	NI-SSMBA	0.554	0.505	0.548	0.556	0.605	0.651	0.606	0.577	—	0.660
	NI-EDA	0.466	0.413	0.460	0.459	0.589	0.587	0.512	0.465	—	0.593
	NI-BT	0.451	0.385	0.447	0.476	0.482	0.501	0.483	0.484	—	0.462
	NI-RandRep	0.323	0.241	0.204	0.306	0.399	0.316	0.253	0.227	—	0.297
	ATC-NE	0.661	0.875	0.901	0.679	0.719	0.867	0.908	0.795	—	0.916
	ATC-MC	0.670	0.874	0.903	0.684	0.729	0.866	0.909	0.801	—	0.916
toys	NI-SSMBA	0.625	0.693	0.656	0.620	0.643	0.661	0.708	0.618	0.650	—
	NI-EDA	0.473	0.582	0.487	0.481	0.498	0.552	0.535	0.429	0.528	—
	NI-BT	0.311	0.408	0.331	0.351	0.324	0.355	0.420	0.334	0.357	—
	NI-RandRep	0.272	0.307	0.234	0.254	0.286	0.257	0.301	0.215	0.248	—
	ATC-NE	0.686	0.936	0.855	0.742	0.712	0.838	0.885	0.561	0.866	—
	ATC-MC	0.691	0.935	0.858	0.742	0.718	0.843	0.886	0.574	0.869	—

Table 12: Full R^2 metrics for all pairs of training and test domains for CNN models trained on AWS.

Train Domain	Measure	Test Domain									
		books	clothing	home	kindle	movies	pets	sports	tech	tools	toys
books	NI-SSMBA	—	0.973	0.983	0.987	0.963	0.973	0.985	0.985	0.977	0.968
	NI-EDA	—	0.961	0.970	0.982	0.966	0.966	0.970	0.957	0.978	0.981
	NI-BT	—	0.946	0.979	0.985	0.961	0.972	0.972	0.975	0.970	0.955
	NI-RandRep	—	0.956	0.970	0.981	0.958	0.967	0.970	0.973	0.952	0.961
	ATC-NE	—	0.845	0.861	0.957	0.927	0.940	0.852	0.925	0.853	0.876
	ATC-MC	—	0.838	0.842	0.947	0.924	0.929	0.840	0.927	0.845	0.876
clothing	NI-SSMBA	0.944	—	0.974	0.942	0.980	0.981	0.984	0.973	0.969	0.978
	NI-EDA	0.974	—	0.970	0.922	0.955	0.978	0.961	0.971	0.953	0.972
	NI-BT	0.944	—	0.977	0.921	0.971	0.983	0.982	0.980	0.970	0.993
	NI-RandRep	0.950	—	0.965	0.933	0.982	0.977	0.985	0.981	0.974	0.973
	ATC-NE	0.792	—	0.934	0.764	0.913	0.939	0.933	0.846	0.914	0.973
	ATC-MC	0.801	—	0.945	0.789	0.917	0.948	0.933	0.887	0.926	0.971
home	NI-SSMBA	0.973	0.972	—	0.976	0.972	0.979	0.976	0.980	0.972	0.984
	NI-EDA	0.961	0.975	—	0.967	0.959	0.960	0.949	0.917	0.963	0.979
	NI-BT	0.947	0.958	—	0.944	0.947	0.948	0.977	0.972	0.971	0.974
	NI-RandRep	0.978	0.976	—	0.970	0.967	0.975	0.973	0.964	0.975	0.983
	ATC-NE	0.878	0.959	—	0.958	0.908	0.930	0.962	0.860	0.928	0.951
	ATC-MC	0.885	0.960	—	0.963	0.913	0.945	0.964	0.872	0.938	0.952
kindle	NI-SSMBA	0.992	0.963	0.966	—	0.961	0.957	0.963	0.971	0.943	0.984
	NI-EDA	0.983	0.968	0.951	—	0.966	0.962	0.953	0.974	0.963	0.969
	NI-BT	0.973	0.947	0.975	—	0.954	0.949	0.954	0.973	0.923	0.973
	NI-RandRep	0.979	0.946	0.956	—	0.967	0.961	0.946	0.970	0.934	0.975
	ATC-NE	0.931	0.380	0.510	—	0.861	0.162	0.260	0.424	0.179	0.608
	ATC-MC	0.930	0.534	0.623	—	0.871	0.294	0.392	0.551	0.316	0.672
movies	NI-SSMBA	0.984	0.976	0.969	0.981	—	0.962	0.983	0.958	0.961	0.971
	NI-EDA	0.974	0.975	0.947	0.985	—	0.928	0.977	0.950	0.972	0.969
	NI-BT	0.971	0.952	0.965	0.965	—	0.951	0.970	0.957	0.950	0.977
	NI-RandRep	0.981	0.969	0.954	0.971	—	0.958	0.969	0.957	0.958	0.962
	ATC-NE	0.948	0.864	0.902	0.949	—	0.746	0.908	0.813	0.817	0.917
	ATC-MC	0.949	0.893	0.928	0.948	—	0.802	0.929	0.861	0.859	0.926
pets	NI-SSMBA	0.943	0.974	0.981	0.945	0.942	—	0.979	0.982	0.978	0.969
	NI-EDA	0.965	0.980	0.985	0.958	0.952	—	0.983	0.975	0.976	0.983
	NI-BT	0.936	0.971	0.974	0.931	0.926	—	0.980	0.963	0.979	0.977
	NI-RandRep	0.941	0.976	0.971	0.925	0.931	—	0.976	0.968	0.976	0.979
	ATC-NE	0.594	0.967	0.900	0.577	0.862	—	0.947	0.959	0.929	0.882
	ATC-MC	0.611	0.968	0.909	0.589	0.851	—	0.955	0.959	0.939	0.894
sports	NI-SSMBA	0.979	0.982	0.994	0.980	0.979	0.970	—	0.982	0.984	0.978
	NI-EDA	0.979	0.987	0.986	0.960	0.984	0.985	—	0.985	0.986	0.987
	NI-BT	0.966	0.977	0.989	0.949	0.969	0.979	—	0.986	0.984	0.988
	NI-RandRep	0.981	0.979	0.994	0.978	0.980	0.978	—	0.985	0.985	0.984
	ATC-NE	0.655	0.945	0.963	0.688	0.850	0.890	—	0.938	0.969	0.957
	ATC-MC	0.705	0.951	0.965	0.722	0.882	0.905	—	0.944	0.972	0.953
tech	NI-SSMBA	0.944	0.979	0.977	0.947	0.967	0.958	0.975	—	0.990	0.981
	NI-EDA	0.917	0.969	0.971	0.925	0.953	0.937	0.967	—	0.963	0.972
	NI-BT	0.894	0.982	0.987	0.924	0.937	0.933	0.978	—	0.987	0.972
	NI-RandRep	0.929	0.959	0.977	0.918	0.952	0.944	0.963	—	0.984	0.971
	ATC-NE	0.937	0.939	0.983	0.933	0.946	0.961	0.961	—	0.974	0.981
	ATC-MC	0.941	0.941	0.980	0.928	0.955	0.958	0.963	—	0.971	0.982
tools	NI-SSMBA	0.977	0.988	0.975	0.967	0.971	0.986	0.985	0.978	—	0.983
	NI-EDA	0.975	0.985	0.978	0.969	0.980	0.986	0.988	0.975	—	0.982
	NI-BT	0.940	0.976	0.970	0.941	0.944	0.969	0.978	0.948	—	0.975
	NI-RandRep	0.963	0.985	0.978	0.954	0.963	0.988	0.984	0.977	—	0.987
	ATC-NE	0.857	0.945	0.964	0.883	0.865	0.925	0.964	0.963	—	0.922
	ATC-MC	0.868	0.941	0.965	0.887	0.876	0.936	0.967	0.971	—	0.919
toys	NI-SSMBA	0.955	0.971	0.985	0.980	0.961	0.966	0.988	0.978	0.971	—
	NI-EDA	0.965	0.968	0.984	0.970	0.985	0.973	0.981	0.975	0.983	—
	NI-BT	0.890	0.946	0.959	0.944	0.925	0.935	0.965	0.943	0.934	—
	NI-RandRep	0.959	0.970	0.979	0.960	0.965	0.967	0.977	0.978	0.974	—
	ATC-NE	0.883	0.878	0.885	0.763	0.906	0.798	0.938	0.815	0.899	—
	ATC-MC	0.889	0.897	0.895	0.754	0.920	0.818	0.947	0.833	0.914	—

Table 13: Full R^2 metrics for all pairs of training and test domains for BERT models trained on AWS.

Train Domain	Measure	Test Domain									
		slate	verbatim	facetoface	oup	nineeleven	fiction	telephone	travel	letters	government
slate	NI-SSMBA	—	0.457	0.760	0.544	0.642	0.706	0.727	0.585	0.640	0.714
	NI-EDA	—	0.574	0.723	0.565	0.620	0.708	0.731	0.549	0.595	0.706
	NI-BT	—	0.862	0.920	0.942	0.930	0.913	0.878	0.936	0.949	0.940
	NI-RandRep	—	0.242	0.336	0.501	0.415	0.121	0.170	0.301	0.652	0.470
	ATC-NE	—	0.681	0.677	0.594	0.599	0.741	0.669	0.664	0.661	0.773
	ATC-MC	—	0.682	0.675	0.590	0.600	0.737	0.670	0.665	0.661	0.771
fiction	NI-SSMBA	0.581	0.492	0.765	0.451	0.530	—	0.683	0.499	0.502	0.614
	NI-EDA	0.657	0.601	0.728	0.620	0.530	—	0.676	0.527	0.508	0.642
	NI-BT	0.889	0.887	0.917	0.950	0.921	—	0.863	0.928	0.935	0.941
	NI-RandRep	0.360	0.414	0.459	0.666	0.531	—	0.188	0.464	0.680	0.631
	ATC-NE	0.530	0.425	0.718	0.323	0.536	—	0.556	0.425	0.597	0.522
	ATC-MC	0.525	0.418	0.719	0.326	0.534	—	0.555	0.422	0.592	0.521
telephone	NI-SSMBA	0.539	0.453	0.826	0.429	0.480	0.647	—	0.436	0.559	0.439
	NI-EDA	0.677	0.636	0.804	0.492	0.639	0.819	—	0.557	0.653	0.568
	NI-BT	0.882	0.901	0.928	0.936	0.927	0.912	—	0.937	0.916	0.919
	NI-RandRep	0.332	0.498	0.488	0.584	0.538	0.310	—	0.586	0.677	0.576
	ATC-NE	0.557	0.518	0.762	0.527	0.467	0.695	—	0.368	0.554	0.468
	ATC-MC	0.561	0.518	0.762	0.524	0.467	0.698	—	0.372	0.560	0.470
travel	NI-SSMBA	0.503	0.506	0.588	0.419	0.501	0.543	0.597	—	0.670	0.507
	NI-EDA	0.444	0.429	0.502	0.388	0.342	0.532	0.478	—	0.438	0.377
	NI-BT	0.806	0.799	0.861	0.916	0.889	0.828	0.802	—	0.923	0.907
	NI-RandRep	0.315	0.333	0.385	0.643	0.516	0.182	0.224	—	0.690	0.626
	ATC-NE	0.561	0.516	0.498	0.686	0.546	0.581	0.606	—	0.585	0.598
	ATC-MC	0.563	0.517	0.503	0.690	0.544	0.588	0.611	—	0.582	0.607
government	NI-SSMBA	0.592	0.497	0.618	0.572	0.596	0.648	0.593	0.539	0.676	—
	NI-EDA	0.577	0.574	0.550	0.476	0.618	0.600	0.491	0.518	0.526	—
	NI-BT	0.818	0.812	0.859	0.909	0.893	0.813	0.809	0.909	0.917	—
	NI-RandRep	0.010	0.083	0.207	0.306	0.279	0.011	0.027	0.123	0.360	—
	ATC-NE	0.663	0.405	0.564	0.722	0.337	0.634	0.630	0.509	0.653	—
	ATC-MC	0.666	0.405	0.574	0.721	0.341	0.633	0.636	0.509	0.654	—

Table 14: Full R^2 metrics for all pairs of training and test domains for CNN models trained on MNLI.

Train Domain	Measure	Test Domain									
		slate	verbatim	facetoface	oup	nineeleven	fiction	telephone	travel	letters	government
slate	NI-SSMBA	—	0.920	0.905	0.943	0.916	0.929	0.930	0.957	0.931	0.970
	NI-EDA	—	0.701	0.754	0.816	0.784	0.790	0.708	0.787	0.820	0.837
	NI-BT	—	0.862	0.920	0.942	0.930	0.913	0.878	0.936	0.949	0.940
	NI-RandRep	—	0.242	0.336	0.501	0.415	0.121	0.170	0.301	0.652	0.470
	ATC-NE	—	0.878	0.899	0.954	0.911	0.925	0.911	0.904	0.890	0.951
	ATC-MC	—	0.871	0.884	0.953	0.908	0.932	0.914	0.911	0.887	0.949
fiction	NI-SSMBA	0.954	0.928	0.895	0.952	0.946	—	0.952	0.975	0.946	0.954
	NI-EDA	0.661	0.687	0.699	0.840	0.686	—	0.683	0.764	0.799	0.797
	NI-BT	0.889	0.887	0.917	0.950	0.921	—	0.863	0.928	0.935	0.941
	NI-RandRep	0.360	0.414	0.459	0.666	0.531	—	0.188	0.464	0.680	0.631
	ATC-NE	0.808	0.585	0.881	0.726	0.939	—	0.836	0.826	0.850	0.890
	ATC-MC	0.817	0.652	0.889	0.732	0.936	—	0.841	0.830	0.861	0.892
telephone	NI-SSMBA	0.943	0.962	0.948	0.953	0.917	0.954	—	0.921	0.934	0.956
	NI-EDA	0.776	0.787	0.790	0.852	0.823	0.847	—	0.853	0.877	0.852
	NI-BT	0.882	0.901	0.928	0.936	0.927	0.912	—	0.937	0.916	0.919
	NI-RandRep	0.332	0.498	0.488	0.584	0.538	0.310	—	0.586	0.677	0.576
	ATC-NE	0.662	0.576	0.884	0.904	0.762	0.665	—	0.771	0.856	0.889
	ATC-MC	0.714	0.668	0.902	0.924	0.807	0.732	—	0.795	0.857	0.899
travel	NI-SSMBA	0.938	0.935	0.949	0.924	0.948	0.946	0.958	—	0.962	0.953
	NI-EDA	0.538	0.553	0.471	0.711	0.602	0.638	0.533	—	0.755	0.699
	NI-BT	0.806	0.799	0.861	0.916	0.889	0.828	0.802	—	0.923	0.907
	NI-RandRep	0.315	0.333	0.385	0.643	0.516	0.182	0.224	—	0.690	0.626
	ATC-NE	0.319	0.417	0.500	0.889	0.768	0.396	0.494	—	0.928	0.911
	ATC-MC	0.412	0.506	0.591	0.906	0.789	0.525	0.572	—	0.921	0.917
government	NI-SSMBA	0.916	0.960	0.781	0.919	0.816	0.882	0.914	0.950	0.920	—
	NI-EDA	0.484	0.572	0.544	0.728	0.715	0.655	0.566	0.644	0.681	—
	NI-BT	0.818	0.812	0.859	0.909	0.893	0.813	0.809	0.909	0.917	—
	NI-RandRep	0.010	0.083	0.207	0.306	0.279	0.011	0.027	0.123	0.360	—
	ATC-NE	0.544	0.385	0.439	0.914	0.731	0.157	0.449	0.538	0.842	—
	ATC-MC	0.624	0.481	0.478	0.919	0.797	0.243	0.505	0.576	0.856	—

Table 15: Full R^2 metrics for all pairs of training and test domains for BERT models trained on MNLI.

Measure	Test Domain						
	ImageNetV2	ImagenNet-Sketch	ObjectNet	ImageNet-Vid	YTBB	ImageNet-R	ImageNet-A
NI-RandAug	0.816	0.677	0.646	0.790	0.692	0.724	0.586
NI-Translate	0.785	0.515	0.516	0.685	0.544	0.581	0.439
NI-Erase	0.779	0.322	0.52	0.706	0.560	0.444	0.517
NI-FC	0.842	0.552	0.645	0.780	0.649	0.679	0.589
ATC-MC	0.891	0.708	0.756	0.761	0.509	0.521	0.190
ATC-NE	0.926	0.717	0.671	0.651	0.494	0.569	0.248

Table 16: Full macro τ metrics for all ImageNet test domains. We average values across models.

Model	Train Domain	Measure	Test Domain		
			SVHN	Colored MNIST	MNIST
NiN	SVHN	NI-RandAug	—	0.668	0.616
		NI-Translate	—	0.699	0.635
		NI-Erase	—	-0.102	-0.168
		NI-FC	—	-0.233	-0.398
		ATC-NE	—	0.577	0.695
		ATC-MC	—	0.646	0.716

Table 17: Full macro τ metrics for all test domains for image classification models on SVHN, Colored MNIST, and MNIST.

Model	Train Domain	Measure	Test Domain			
			CIFAR10	CINIC10	CIFAR10.1	CIFAR10.2
NiN	CIFAR10	NI-RandAug	—	0.785	0.830	0.783
		NI-Translate	—	0.621	0.739	0.644
		NI-Erase	—	0.385	0.485	0.499
		NI-FC	—	0.194	0.077	-0.037
		ATC-NE	—	0.250	0.543	0.484
		ATC-MC	—	0.319	0.514	0.446
ResNet	CIFAR10	NI-RandAug	—	0.706	0.722	0.742
		NI-Translate	—	0.800	0.796	0.741
		NI-Erase	—	0.723	0.727	0.699
		NI-FC	—	0.647	0.585	0.607
		ATC-NE	—	0.644	0.687	0.630
		ATC-MC	—	0.631	0.672	0.624
VGG	CIFAR10	NI-RandAug	—	0.868	0.831	0.772
		NI-Translate	—	0.700	0.679	0.632
		NI-Erase	—	-0.153	-0.196	-0.215
		NI-FC	—	0.597	0.569	0.512
		ATC-NE	—	0.531	0.656	0.599
		ATC-MC	—	0.533	0.648	0.586
CNN	CINIC10	NI-RandAug	0.756	—	0.698	0.695
		NI-Translate	0.347	—	0.318	0.267
		NI-Erase	0.619	—	0.539	0.577
		NI-FC	0.249	—	0.286	0.252
		ATC-NE	0.607	—	0.510	0.447
		ATC-MC	0.611	—	0.500	0.440

Table 18: Full macro τ metrics for all test domains for image classification models on CIFAR10, CINIC10, CIFAR10.1, and CIFAR10.2.

Train Domain	Measure	Test Domain									
		books	clothing	home	kindle	movies	pets	sports	tech	tools	toys
books	NI-SSMBA	—	0.708	0.741	0.687	0.678	0.754	0.738	0.738	0.721	0.669
	NI-EDA	—	0.722	0.738	0.640	0.685	0.756	0.688	0.709	0.719	0.725
	NI-BT	—	0.615	0.631	0.549	0.596	0.656	0.602	0.644	0.584	0.621
	NI-RandRep	—	0.591	0.586	0.499	0.587	0.587	0.530	0.530	0.546	0.589
	ATC-NE	—	0.605	0.642	0.534	0.496	0.629	0.605	0.538	0.618	0.673
	ATC-MC	—	0.604	0.639	0.534	0.489	0.630	0.606	0.544	0.616	0.670
clothing	NI-SSMBA	0.769	—	0.774	0.773	0.793	0.726	0.653	0.716	0.692	0.709
	NI-EDA	0.681	—	0.670	0.787	0.721	0.696	0.675	0.694	0.690	0.784
	NI-BT	0.574	—	0.542	0.654	0.595	0.481	0.506	0.501	0.503	0.679
	NI-RandRep	0.623	—	0.591	0.603	0.612	0.557	0.496	0.507	0.549	0.640
	ATC-NE	0.420	—	0.366	0.408	0.450	0.308	0.501	0.242	0.560	0.563
	ATC-MC	0.421	—	0.363	0.409	0.451	0.315	0.498	0.239	0.558	0.563
home	NI-SSMBA	0.786	0.552	—	0.731	0.731	0.769	0.790	0.789	0.775	0.614
	NI-EDA	0.734	0.659	—	0.767	0.649	0.757	0.707	0.723	0.696	0.748
	NI-BT	0.670	0.498	—	0.641	0.639	0.634	0.706	0.688	0.662	0.630
	NI-RandRep	0.700	0.549	—	0.665	0.705	0.686	0.663	0.664	0.632	0.651
	ATC-NE	0.450	0.480	—	0.459	0.447	0.455	0.559	0.497	0.558	0.445
	ATC-MC	0.459	0.480	—	0.460	0.452	0.458	0.557	0.495	0.557	0.448
kindle	NI-SSMBA	0.546	0.679	0.648	—	0.557	0.699	0.656	0.608	0.607	0.630
	NI-EDA	0.663	0.644	0.717	—	0.637	0.743	0.699	0.676	0.643	0.696
	NI-BT	0.556	0.648	0.652	—	0.562	0.686	0.683	0.668	0.643	0.674
	NI-RandRep	0.454	0.519	0.406	—	0.428	0.555	0.434	0.415	0.415	0.535
	ATC-NE	0.370	0.517	0.468	—	0.338	0.583	0.540	0.383	0.472	0.545
	ATC-MC	0.388	0.512	0.469	—	0.342	0.578	0.538	0.384	0.467	0.541
movies	NI-SSMBA	0.572	0.689	0.717	0.660	—	0.732	0.741	0.675	0.714	0.749
	NI-EDA	0.500	0.717	0.711	0.629	—	0.733	0.725	0.660	0.719	0.748
	NI-BT	0.619	0.681	0.687	0.595	—	0.738	0.729	0.717	0.717	0.717
	NI-RandRep	0.435	0.491	0.523	0.554	—	0.460	0.528	0.436	0.517	0.570
	ATC-NE	0.436	0.605	0.623	0.398	—	0.571	0.622	0.502	0.659	0.701
	ATC-MC	0.449	0.612	0.631	0.403	—	0.586	0.628	0.520	0.661	0.704
pets	NI-SSMBA	0.747	0.560	0.653	0.766	0.769	—	0.719	0.696	0.697	0.731
	NI-EDA	0.762	0.684	0.682	0.794	0.773	—	0.709	0.666	0.689	0.745
	NI-BT	0.741	0.550	0.625	0.751	0.776	—	0.704	0.676	0.702	0.654
	NI-RandRep	0.619	0.575	0.572	0.696	0.662	—	0.580	0.532	0.590	0.710
	ATC-NE	0.570	0.545	0.462	0.533	0.543	—	0.511	0.333	0.503	0.634
	ATC-MC	0.575	0.541	0.461	0.535	0.546	—	0.510	0.332	0.502	0.632
sports	NI-SSMBA	0.774	0.561	0.657	0.812	0.764	0.683	—	0.689	0.746	0.651
	NI-EDA	0.770	0.633	0.659	0.791	0.710	0.712	—	0.701	0.732	0.692
	NI-BT	0.670	0.484	0.598	0.669	0.672	0.545	—	0.534	0.704	0.538
	NI-RandRep	0.684	0.472	0.562	0.704	0.638	0.589	—	0.614	0.622	0.693
	ATC-NE	0.502	0.456	0.454	0.506	0.443	0.374	—	0.397	0.565	0.577
	ATC-MC	0.513	0.459	0.459	0.521	0.453	0.393	—	0.410	0.574	0.574
tech	NI-SSMBA	0.784	0.674	0.768	0.793	0.779	0.755	0.785	—	0.690	0.746
	NI-EDA	0.718	0.698	0.760	0.743	0.752	0.817	0.772	—	0.726	0.781
	NI-BT	0.715	0.576	0.719	0.732	0.746	0.716	0.726	—	0.687	0.683
	NI-RandRep	0.680	0.647	0.652	0.686	0.668	0.677	0.664	—	0.553	0.742
	ATC-NE	0.547	0.688	0.681	0.560	0.640	0.653	0.666	—	0.637	0.723
	ATC-MC	0.553	0.690	0.678	0.567	0.639	0.650	0.664	—	0.633	0.721
tools	NI-SSMBA	0.783	0.541	0.604	0.777	0.782	0.757	0.758	0.730	—	0.682
	NI-EDA	0.716	0.544	0.628	0.769	0.735	0.764	0.722	0.696	—	0.745
	NI-BT	0.691	0.342	0.454	0.681	0.677	0.567	0.575	0.636	—	0.513
	NI-RandRep	0.661	0.550	0.581	0.675	0.685	0.668	0.623	0.584	—	0.687
	ATC-NE	0.621	0.472	0.480	0.647	0.648	0.536	0.598	0.448	—	0.619
	ATC-MC	0.630	0.465	0.491	0.649	0.655	0.538	0.597	0.456	—	0.622
toys	NI-SSMBA	0.760	0.702	0.758	0.763	0.731	0.775	0.782	0.750	0.753	—
	NI-EDA	0.689	0.678	0.661	0.757	0.646	0.736	0.711	0.661	0.700	—
	NI-BT	0.582	0.604	0.683	0.626	0.610	0.695	0.723	0.660	0.658	—
	NI-RandRep	0.629	0.660	0.575	0.661	0.609	0.605	0.599	0.543	0.582	—
	ATC-NE	0.401	0.617	0.309	0.479	0.370	0.323	0.485	0.143	0.526	—
	ATC-MC	0.408	0.614	0.315	0.476	0.368	0.329	0.488	0.146	0.535	—

Table 19: Full macro τ metrics for all pairs of training and test domains for CNN models trained on AWS.

Train Domain	Measure	Test Domain									
		books	clothing	home	kindle	movies	pets	sports	tech	tools	toys
books	NI-SSMBA	—	0.886	0.906	0.893	0.901	0.900	0.925	0.918	0.931	0.857
	NI-EDA	—	0.883	0.851	0.890	0.852	0.863	0.854	0.855	0.895	0.844
	NI-BT	—	0.830	0.887	0.893	0.883	0.884	0.871	0.878	0.869	0.824
	NI-RandRep	—	0.882	0.871	0.908	0.906	0.897	0.894	0.900	0.913	0.846
	ATC-NE	—	0.803	0.814	0.851	0.821	0.885	0.756	0.843	0.774	0.832
	ATC-MC	—	0.789	0.806	0.850	0.794	0.874	0.760	0.845	0.768	0.824
clothing	NI-SSMBA	0.797	—	0.882	0.714	0.773	0.826	0.881	0.826	0.883	0.824
	NI-EDA	0.828	—	0.848	0.813	0.787	0.862	0.741	0.839	0.848	0.777
	NI-BT	0.817	—	0.903	0.686	0.837	0.832	0.849	0.835	0.823	0.778
	NI-RandRep	0.762	—	0.858	0.691	0.826	0.832	0.872	0.822	0.868	0.786
	ATC-NE	0.729	—	0.805	0.672	0.681	0.817	0.728	0.698	0.792	0.791
	ATC-MC	0.735	—	0.794	0.683	0.701	0.858	0.744	0.736	0.808	0.791
home	NI-SSMBA	0.736	0.800	—	0.786	0.780	0.868	0.896	0.876	0.888	0.885
	NI-EDA	0.680	0.885	—	0.768	0.830	0.880	0.879	0.843	0.877	0.930
	NI-BT	0.749	0.788	—	0.756	0.778	0.819	0.871	0.835	0.906	0.866
	NI-RandRep	0.729	0.811	—	0.701	0.759	0.853	0.931	0.831	0.876	0.874
	ATC-NE	0.691	0.788	—	0.750	0.802	0.791	0.797	0.739	0.824	0.824
	ATC-MC	0.684	0.782	—	0.738	0.793	0.806	0.772	0.751	0.826	0.819
kindle	NI-SSMBA	0.735	0.850	0.885	—	0.701	0.913	0.875	0.869	0.763	0.871
	NI-EDA	0.840	0.830	0.824	—	0.709	0.879	0.856	0.865	0.854	0.790
	NI-BT	0.727	0.848	0.892	—	0.763	0.856	0.926	0.871	0.879	0.861
	NI-RandRep	0.773	0.848	0.816	—	0.735	0.875	0.857	0.843	0.794	0.847
	ATC-NE	0.695	0.335	0.486	—	0.644	0.211	0.274	0.426	0.238	0.589
	ATC-MC	0.729	0.455	0.558	—	0.671	0.337	0.366	0.509	0.369	0.652
movies	NI-SSMBA	0.845	0.897	0.888	0.782	—	0.850	0.931	0.877	0.881	0.896
	NI-EDA	0.764	0.881	0.852	0.863	—	0.859	0.901	0.863	0.882	0.938
	NI-BT	0.810	0.894	0.882	0.719	—	0.837	0.894	0.864	0.872	0.870
	NI-RandRep	0.851	0.875	0.855	0.742	—	0.850	0.905	0.864	0.861	0.874
	ATC-NE	0.692	0.745	0.807	0.712	—	0.561	0.768	0.580	0.620	0.763
	ATC-MC	0.698	0.770	0.847	0.722	—	0.622	0.813	0.637	0.678	0.784
pets	NI-SSMBA	0.728	0.737	0.866	0.737	0.829	—	0.883	0.867	0.859	0.773
	NI-EDA	0.732	0.831	0.880	0.601	0.788	—	0.853	0.834	0.903	0.841
	NI-BT	0.697	0.685	0.816	0.758	0.816	—	0.867	0.814	0.865	0.810
	NI-RandRep	0.753	0.731	0.813	0.735	0.841	—	0.828	0.871	0.869	0.774
	ATC-NE	0.623	0.740	0.719	0.553	0.737	—	0.815	0.788	0.748	0.781
	ATC-MC	0.662	0.753	0.723	0.566	0.711	—	0.831	0.781	0.752	0.750
sports	NI-SSMBA	0.715	0.743	0.879	0.764	0.837	0.863	—	0.879	0.860	0.870
	NI-EDA	0.757	0.731	0.807	0.673	0.798	0.786	—	0.815	0.827	0.833
	NI-BT	0.728	0.753	0.766	0.664	0.826	0.832	—	0.783	0.824	0.865
	NI-RandRep	0.735	0.702	0.816	0.728	0.808	0.802	—	0.830	0.849	0.836
	ATC-NE	0.489	0.734	0.738	0.567	0.720	0.726	—	0.726	0.725	0.862
	ATC-MC	0.484	0.728	0.766	0.562	0.754	0.727	—	0.725	0.741	0.860
tech	NI-SSMBA	0.784	0.763	0.845	0.710	0.769	0.853	0.755	—	0.886	0.877
	NI-EDA	0.771	0.867	0.881	0.763	0.801	0.855	0.886	—	0.904	0.869
	NI-BT	0.753	0.750	0.867	0.719	0.805	0.869	0.787	—	0.842	0.835
	NI-RandRep	0.819	0.721	0.843	0.711	0.854	0.889	0.787	—	0.854	0.874
	ATC-NE	0.737	0.744	0.787	0.751	0.732	0.795	0.727	—	0.830	0.863
	ATC-MC	0.771	0.730	0.764	0.749	0.704	0.809	0.771	—	0.789	0.843
tools	NI-SSMBA	0.792	0.854	0.786	0.707	0.746	0.875	0.888	0.792	—	0.866
	NI-EDA	0.859	0.846	0.834	0.847	0.790	0.837	0.886	0.819	—	0.894
	NI-BT	0.769	0.802	0.763	0.709	0.750	0.832	0.824	0.744	—	0.856
	NI-RandRep	0.792	0.825	0.816	0.717	0.724	0.885	0.877	0.801	—	0.845
	ATC-NE	0.745	0.789	0.775	0.744	0.632	0.698	0.856	0.737	—	0.799
	ATC-MC	0.749	0.798	0.772	0.745	0.634	0.737	0.876	0.777	—	0.793
toys	NI-SSMBA	0.779	0.830	0.813	0.766	0.695	0.808	0.872	0.872	0.891	—
	NI-EDA	0.696	0.790	0.805	0.821	0.790	0.837	0.834	0.860	0.840	—
	NI-BT	0.748	0.762	0.746	0.755	0.707	0.840	0.809	0.773	0.811	—
	NI-RandRep	0.813	0.788	0.783	0.770	0.660	0.788	0.838	0.873	0.891	—
	ATC-NE	0.656	0.469	0.743	0.550	0.628	0.515	0.792	0.703	0.771	—
	ATC-MC	0.694	0.482	0.726	0.539	0.651	0.571	0.805	0.730	0.777	—

Table 20: Full macro τ metrics for all pairs of training and test domains for BERT models trained on AWS.

Train Domain	Measure	Test Domain									
		slate	verbatim	facetoface	oup	nineeleven	fiction	telephone	travel	letters	government
slate	NI-SSMBA	—	0.483	0.675	0.553	0.608	0.650	0.661	0.570	0.622	0.641
	NI-EDA	—	0.564	0.675	0.563	0.599	0.658	0.672	0.557	0.599	0.649
	NI-BT	—	0.669	0.742	0.736	0.756	0.727	0.754	0.751	0.738	0.791
	NI-RandRep	—	0.393	0.526	0.529	0.480	0.398	0.438	0.445	0.640	0.531
	ATC-NE	—	0.650	0.632	0.577	0.594	0.683	0.625	0.602	0.621	0.699
	ATC-MC	—	0.652	0.632	0.578	0.594	0.681	0.625	0.603	0.622	0.697
fiction	NI-SSMBA	0.577	0.537	0.692	0.482	0.539	—	0.629	0.520	0.546	0.598
	NI-EDA	0.632	0.584	0.691	0.608	0.557	—	0.631	0.529	0.540	0.608
	NI-BT	0.783	0.704	0.771	0.693	0.671	—	0.776	0.680	0.707	0.693
	NI-RandRep	0.495	0.446	0.522	0.531	0.437	—	0.434	0.464	0.531	0.493
	ATC-NE	0.538	0.461	0.630	0.428	0.513	—	0.542	0.469	0.581	0.536
	ATC-MC	0.530	0.450	0.631	0.427	0.513	—	0.543	0.463	0.576	0.534
telephone	NI-SSMBA	0.567	0.503	0.736	0.493	0.507	0.608	—	0.492	0.572	0.496
	NI-EDA	0.637	0.633	0.726	0.537	0.615	0.735	—	0.579	0.642	0.580
	NI-BT	0.657	0.668	0.722	0.637	0.663	0.639	—	0.621	0.602	0.614
	NI-RandRep	0.504	0.470	0.573	0.470	0.510	0.480	—	0.482	0.576	0.440
	ATC-NE	0.533	0.507	0.681	0.526	0.500	0.632	—	0.453	0.564	0.491
	ATC-MC	0.534	0.507	0.681	0.522	0.501	0.637	—	0.455	0.564	0.494
travel	NI-SSMBA	0.524	0.528	0.585	0.462	0.517	0.537	0.569	—	0.617	0.521
	NI-EDA	0.492	0.484	0.523	0.461	0.418	0.550	0.524	—	0.507	0.458
	NI-BT	0.619	0.634	0.630	0.660	0.681	0.655	0.645	—	0.713	0.699
	NI-RandRep	0.465	0.476	0.467	0.514	0.492	0.472	0.526	—	0.569	0.497
	ATC-NE	0.579	0.528	0.533	0.643	0.541	0.571	0.591	—	0.572	0.597
	ATC-MC	0.576	0.528	0.534	0.642	0.536	0.573	0.594	—	0.570	0.602
government	NI-SSMBA	0.578	0.531	0.600	0.568	0.565	0.617	0.589	0.563	0.616	—
	NI-EDA	0.581	0.582	0.565	0.535	0.594	0.624	0.519	0.552	0.566	—
	NI-BT	0.719	0.693	0.686	0.687	0.755	0.701	0.651	0.712	0.719	—
	NI-RandRep	0.274	0.268	0.357	0.444	0.464	0.301	0.247	0.395	0.452	—
	ATC-NE	0.624	0.464	0.581	0.666	0.440	0.601	0.616	0.524	0.641	—
	ATC-MC	0.621	0.465	0.583	0.667	0.446	0.602	0.616	0.522	0.642	—

Table 21: Full macro τ metrics for all pairs of training and test domains for CNN models trained on MNLI.

Train Domain	Measure	Test Domain									
		slate	verbatim	facetoface	oup	nineelevel	fiction	telephone	travel	letters	government
slate	NI-SSMBA	—	0.743	0.746	0.709	0.767	0.742	0.727	0.771	0.782	0.819
	NI-EDA	—	0.580	0.695	0.674	0.696	0.703	0.655	0.651	0.671	0.737
	NI-BT	—	0.669	0.742	0.736	0.756	0.727	0.754	0.751	0.738	0.791
	NI-RandRep	—	0.393	0.526	0.529	0.480	0.398	0.438	0.445	0.640	0.531
	ATC-NE	—	0.689	0.768	0.786	0.728	0.752	0.761	0.744	0.743	0.766
	ATC-MC	—	0.684	0.761	0.794	0.730	0.761	0.789	0.765	0.744	0.785
fiction	NI-SSMBA	0.755	0.673	0.699	0.726	0.729	—	0.769	0.806	0.770	0.727
	NI-EDA	0.609	0.505	0.649	0.659	0.532	—	0.608	0.554	0.624	0.629
	NI-BT	0.783	0.704	0.771	0.693	0.671	—	0.776	0.680	0.707	0.693
	NI-RandRep	0.495	0.446	0.522	0.531	0.437	—	0.434	0.464	0.531	0.493
	ATC-NE	0.618	0.377	0.707	0.478	0.711	—	0.596	0.558	0.658	0.711
	ATC-MC	0.631	0.422	0.702	0.513	0.707	—	0.603	0.549	0.670	0.706
telephone	NI-SSMBA	0.720	0.768	0.793	0.792	0.668	0.720	—	0.813	0.758	0.788
	NI-EDA	0.670	0.667	0.706	0.617	0.718	0.795	—	0.642	0.732	0.661
	NI-BT	0.657	0.668	0.722	0.637	0.663	0.639	—	0.621	0.602	0.614
	NI-RandRep	0.504	0.470	0.573	0.470	0.510	0.480	—	0.482	0.576	0.440
	ATC-NE	0.462	0.486	0.692	0.575	0.641	0.542	—	0.644	0.697	0.702
	ATC-MC	0.519	0.551	0.717	0.641	0.637	0.597	—	0.665	0.684	0.708
travel	NI-SSMBA	0.700	0.806	0.737	0.676	0.744	0.707	0.848	—	0.789	0.783
	NI-EDA	0.483	0.453	0.486	0.493	0.489	0.515	0.483	—	0.522	0.495
	NI-BT	0.619	0.634	0.630	0.660	0.681	0.655	0.645	—	0.713	0.699
	NI-RandRep	0.465	0.476	0.467	0.514	0.492	0.472	0.526	—	0.569	0.497
	ATC-NE	0.155	0.320	0.234	0.559	0.533	0.146	0.360	—	0.633	0.630
	ATC-MC	0.175	0.370	0.320	0.613	0.576	0.219	0.443	—	0.648	0.646
government	NI-SSMBA	0.769	0.777	0.727	0.652	0.640	0.783	0.784	0.805	0.754	—
	NI-EDA	0.521	0.513	0.480	0.578	0.661	0.657	0.494	0.565	0.598	—
	NI-BT	0.719	0.693	0.686	0.687	0.755	0.701	0.651	0.712	0.719	—
	NI-RandRep	0.274	0.268	0.357	0.444	0.464	0.301	0.247	0.395	0.452	—
	ATC-NE	0.377	0.176	0.472	0.660	0.558	0.239	0.497	0.302	0.638	—
	ATC-MC	0.427	0.231	0.487	0.653	0.600	0.275	0.496	0.323	0.629	—

Table 22: Full macro τ metrics for all pairs of training and test domains for BERT models trained on MNLI.

Model	Measure	Test Domain									
		books	clothing	home	kindle	movies	pets	sports	tech	tools	toys
CNN	NI-SSMBA	0.677	0.688	0.758	0.641	0.691	0.786	0.784	0.758	0.722	0.683
	NI-EDA	0.637	0.672	0.704	0.612	0.658	0.746	0.739	0.680	0.703	0.711
	NI-BT	0.601	0.532	0.572	0.509	0.521	0.509	0.587	0.536	0.571	0.529
	NI-RandRep	0.485	0.542	0.501	0.522	0.440	0.491	0.650	0.477	0.507	0.550
	ATC-NE	0.406	0.727	0.728	0.362	0.499	0.722	0.726	0.679	0.730	0.752
	ATC-MC	0.410	0.726	0.729	0.359	0.500	0.724	0.727	0.681	0.730	0.752
BERT	NI-SSMBA	0.790	0.850	0.868	0.664	0.899	0.864	0.855	0.874	0.880	0.845
	NI-EDA	0.739	0.848	0.825	0.731	0.793	0.836	0.825	0.828	0.837	0.841
	NI-BT	0.702	0.845	0.830	0.668	0.792	0.839	0.843	0.813	0.819	0.858
	NI-RandRep	0.839	0.841	0.891	0.694	0.864	0.834	0.747	0.825	0.850	0.831
	ATC-NE	0.613	0.721	0.712	0.618	0.695	0.666	0.733	0.693	0.708	0.755
	ATC-MC	0.621	0.735	0.730	0.616	0.711	0.691	0.749	0.710	0.726	0.764

Table 23: Full micro τ metrics for all test domains for CNN and BERT models trained on AWS.

Model	Measure	Test Domain									
		slate	verbatim	facetoface	oup	nineeleven	fiction	telephone	travel	letters	government
CNN	NI-SSMBA	0.540	0.493	0.562	0.493	0.527	0.431	0.607	0.544	0.579	0.563
	NI-EDA	0.560	0.555	0.427	0.520	0.488	0.435	0.499	0.552	0.532	0.542
	NI-BT	0.698	0.684	0.611	0.713	0.713	0.595	0.676	0.714	0.697	0.722
	NI-RandRep	0.448	0.417	0.427	0.503	0.472	0.324	0.395	0.450	0.550	0.509
	ATC-NE	0.461	0.413	0.549	0.427	0.350	0.517	0.531	0.307	0.497	0.404
	ATC-MC	0.460	0.411	0.550	0.429	0.351	0.517	0.532	0.307	0.496	0.404
BERT	NI-SSMBA	0.782	0.710	0.742	0.652	0.724	0.756	0.779	0.691	0.768	0.700
	NI-EDA	0.563	0.556	0.481	0.622	0.586	0.545	0.529	0.607	0.607	0.630
	NI-BT	0.698	0.684	0.611	0.713	0.713	0.595	0.676	0.714	0.697	0.722
	NI-RandRep	0.448	0.417	0.427	0.503	0.472	0.324	0.395	0.450	0.550	0.509
	ATC-NE	0.375	0.389	0.660	0.606	0.593	0.414	0.523	0.511	0.655	0.687
	ATC-MC	0.405	0.434	0.676	0.632	0.614	0.466	0.554	0.530	0.663	0.693

Table 24: Full micro τ metrics for all test domains for CNN and BERT models trained on MNLI.

Measure	Train Domain (Model)				
	SVHN (NiN)	CIFAR10 (NiN)	CIFAR10 (ResNet)	CIFAR10 (VGG)	CINIC10 (CNN)
NI-RandAug	0.733	0.797	0.746	0.869	0.759
NI-Translate	0.881	0.782	0.833	0.699	0.329
NI-Erase	0.324	0.409	0.708	-0.183	0.606
NI-FC	-0.033	-0.015	0.568	0.628	0.289
ATC-NE	0.859	0.648	0.757	0.773	0.548
ATC-MC	0.843	0.605	0.756	0.767	0.553

Table 25: Full in-domain τ metrics for all test domains for image classification models and datasets.

Model	Measure	Train Domain									
		books	clothing	home	kindle	movies	pets	sports	tech	tools	toys
CNN	NI-SSMBA	0.646	0.613	0.643	0.577	0.597	0.591	0.703	0.648	0.643	0.620
	NI-EDA	0.653	0.558	0.615	0.660	0.447	0.666	0.708	0.646	0.663	0.565
	NI-BT	0.569	0.449	0.582	0.537	0.626	0.605	0.568	0.653	0.640	0.652
	NI-RandRep	0.560	0.557	0.559	0.559	0.593	0.596	0.572	0.545	0.566	0.615
	ATC-NE	0.575	0.413	0.561	0.478	0.294	0.464	0.539	0.561	0.446	0.341
	ATC-MC	0.566	0.405	0.558	0.478	0.300	0.461	0.540	0.569	0.451	0.338
BERT	NI-SSMBA	0.735	0.874	0.868	0.693	0.780	0.871	0.884	0.851	0.851	0.884
	NI-EDA	0.875	0.788	0.814	0.700	0.870	0.894	0.818	0.858	0.882	0.810
	NI-BT	0.801	0.811	0.857	0.638	0.835	0.813	0.860	0.846	0.803	0.750
	NI-RandRep	0.839	0.841	0.891	0.694	0.864	0.834	0.747	0.825	0.850	0.831
	ATC-NE	0.733	0.724	0.822	0.640	0.721	0.711	0.778	0.783	0.799	0.783
	ATC-MC	0.742	0.746	0.813	0.630	0.730	0.725	0.814	0.780	0.774	0.739

Table 26: Full in-domain τ metrics for all test domains for CNN and BERT models trained on AWS.

Model	Measure	Train Domain				
		slate	fiction	telephone	travel	government
CNN	NI-SSMBA	0.664	0.655	0.753	0.692	0.758
	NI-EDA	0.629	0.723	0.786	0.652	0.755
	NI-BT	0.751	0.765	0.637	0.786	0.826
	NI-RandRep	0.437	0.471	0.546	0.570	0.491
	ATC-NE	0.704	0.662	0.719	0.715	0.722
	ATC-MC	0.703	0.660	0.722	0.716	0.728
BERT	NI-SSMBA	0.713	0.754	0.766	0.785	0.839
	NI-EDA	0.608	0.664	0.781	0.575	0.726
	NI-BT	0.751	0.765	0.637	0.786	0.826
	NI-RandRep	0.437	0.471	0.546	0.570	0.491
	ATC-NE	0.722	0.796	0.740	0.737	0.701
	ATC-MC	0.745	0.791	0.791	0.719	0.696

Table 27: Full in-domain τ metrics for all train domains for CNN and BERT models trained on MNLI.

Measure	Domain Shifts		ImageNet-A		
	R^2	Macro τ	R^2	Macro τ	ID τ
NI-RandAug	0.091	0.061	—	—	—
NI-Translate	0.159	0.099	—	—	—
NI-Erase	0.174	0.153	—	—	—
NI-FC	0.139	0.095	—	—	—
ATC-NE	0.272	0.136	—	—	—
ATC-MC	0.279	0.135	—	—	—

(a) Standard deviations for ImageNet scale results. No standard deviations are reported for ImageNet-A or ID τ since we report only a single value.

Measure	CI10			Numbers		
	R^2	Macro τ	ID τ	R^2	Macro τ	ID τ
NI-RandAug	0.044	0.054	0.048	0.021	0.026	—
NI-Translate	0.170	0.181	0.197	0.043	0.032	—
NI-Erase	0.254	0.348	0.345	0.065	0.033	—
NI-FC	0.239	0.225	0.255	0.074	0.083	—
ATC-NE	0.169	0.115	0.091	0.109	0.059	—
ATC-MC	0.168	0.101	0.093	0.077	0.035	—

(b) Standard deviations for small scale image results. No standard deviation is reported for Numbers ID τ since we report only a single value.

Measure	CNN				RoBERTa			
	R^2	Macro τ	Micro τ	ID τ	R^2	Macro τ	Micro τ	ID τ
NI-SSMBA	0.079	0.067	0.046	0.035	0.012	0.063	0.064	0.065
NI-EDA	0.108	0.051	0.041	0.072	0.016	0.058	0.040	0.055
NI-BT	0.161	0.078	0.032	0.060	0.021	0.060	0.061	0.063
NI-RandRep	0.069	0.080	0.054	0.021	0.015	0.060	0.055	0.055
ATC-NE	0.126	0.110	0.143	0.092	0.168	0.135	0.044	0.051
ATC-MC	0.125	0.109	0.143	0.091	0.139	0.112	0.048	0.050

(c) Standard deviations on sentiment analysis results.

Measure	CNN				RoBERTa			
	R^2	Macro τ	Micro τ	ID τ	R^2	Macro τ	Micro τ	ID τ
NI-SSMBA	0.098	0.060	0.048	0.043	0.035	0.046	0.040	0.041
NI-EDA	0.107	0.068	0.046	0.060	0.108	0.087	0.044	0.075
NI-BT	0.045	0.049	0.042	0.063	0.045	0.049	0.042	0.063
NI-RandRep	0.196	0.079	0.061	0.049	0.196	0.079	0.061	0.049
ATC-NE	0.108	0.068	0.076	0.022	0.206	0.180	0.111	0.032
ATC-MC	0.108	0.068	0.076	0.024	0.174	0.164	0.100	0.038

(d) Standard deviations on NLI results.

Table 28: Standard deviations for reported values in Table 2